An Equipment Protection and Safety System for the ASDEX Tokamak

J.Gernhardt, D.Groening, H.Hohenöcker, N.Ruhs

IPP III/65 February 1981

MAX-PLANCK-INSTITUT FÜR PLASMAPHYSIK

8046 GARCHING BEI MÜNCHEN

MAX-PLANCK-INSTITUT FÜR PLASMAPHYSIK

GARCHING BEI MÜNCHEN

An Equipment Protection and Safety System for the ASDEX Tokamak

J.Gernhardt, D.Groening, H.Hohenöcker, N.Ruhs

IPP III/65 February 1981

Die nachstehende Arbeit wurde im Rahmen des Vertrages zwischen dem Max-Planck-Institut für Plasmaphysik und der Europäischen Atomgemeinschaft über die Zusammenarbeit auf dem Gebiete der Plasmaphysik durchgeführt.

IPP III/65

J.Gernhardt
D.Groening
H.Hohenöcker
N.Ruhs

An Equipment Protection and Safety System for the ASDEX Tokamak

Abstract

Our compromise between safety requirements and costs is a hybrid of relay, solid-state and computer-controlled protection systems /1/ used for ASDEX /2/. The toroidal field coils, ohmic heating coils, vertical field coils, divertor coils, radial field coils, stainless-steel vacuum vessel and structure are protected by measuring the water flow (131 channels), temperature (142 channels), mechanical displacements (141 channels), voltage symmetry (28 channels), current symmetry (6 channels), weight of the vessel (8 channels) and the overvoltage /3/. To detect flow, temperature, displacement, voltage, current and weight, we use the following devices: Venturi tubes (self-made), RTD thermoresistors (Pt-100), linear potentiometers (1 kΩ), voltage dividers (self-made), Rogowski coils (self-made) and strain gauges.

Table of contents

1. Introduction

By writing this paper it was our intention to discuss the following subjects which give a survey of the protection system.

1.1 The temperature measuring system protects the coil system, including coil insulation, coil-contacts and the framework against high temperature.

1.2 The water flow detection system protects the coil systems against high temperature. Some individual channels of protection systems of Sec. 1.1 and 1.2 are redundant.

1.3 The force and displacement measuring systems protect the coil systems against high stress in the copper and copper beryllium windings of coil systems.

1.4 The voltage symmetry measuring system protects the individual coil system against arcing and short circuits. This protection system reduces the extent of destruction depending on the energy content of the coil systems.

1.5 The current symmetry measuring system protects the high current leads of the divertor coils against high forces.

Table IV shows the actions taken on reaching the individual set point limits.

Fig. 1 shows the two completed halves of ASDEX before they are joined together. Near the person in the picture one can see the central column made of special presswood. Because each of the 16 main field coils "generate" a centripetal force of 10 mega newton per coil the central column has to take this force. Inside the wooden central column we mounted 16 linear potentiometers to measure the displacement and two RTD's to measure the temperature 20 and 50 mm inside the wood (wood has low heat conductivity). At the main field coils we measured the displacement in the radial direction at z=0 (see Fig. 39 for notation) between the copper windings and the (stainless steel) coil housing. In the right half of Fig. 1 one can see the inner ohmic heating coils, vertical field and divertor compensation coils where we measured the temperature and displacement /4/. The divertor coil triplets are mounted in the upper and lower parts inside the vacuum vessel /5/.

Fig. 2 shows the simplified upper cross section of ASDEX. It is very difficult without testing to mount the linear potentiometer at those places where the displacement has its maximum. From calculations we knew the radial displacement produced by the thermal radial expansion and magnetic force, but we did not know where the maximum displacement would occur. For this reason we made current tests after mounting the coils in ASDEX. With 60 linear potentiometers that could be changed around we detected the maximum displacements and hence the proper place at which to locate the linear potentiometer for the operating phase of ASDEX. Several tests were made with one coil system and with the combined coil system to find the maximum displacement.

The criterion for any safety system is that it should be automatic and fast and cover all location where dangerous conditions can develop. Furthermore, the safety system has to be safe within itself. This means that common mode voltage, pick-up of magnetic fields or high-voltage spikes make the safety system unsafe and have to be reduced as far as possible. To obtain high reliability we tested the

transducer, cable /6/ and transmitter in a test environment consisting of a high temperature, magnetic field and high voltage. All installed cables are protected against mechanical force by a Teflon or copper tube in the experiment (see Fig. 3 and 4). Between the experiment and the control room (approx. 30 m) we used fire-resisting painted cable ducts made of press wood (area: 40 cm x 15 cm). The 2 or 3 conductors (AWG 24) of the cable are twisted up to 2 twists per cm cable length (to reduce the magnetic pick-up) and shielded by a copper braid and aluminum foil (to reduce electrostatic pick-up). The outside diameter of each symmetrically twisted cable is ≤ 4 mm to fit in Lemosa connectors size No. 0 or No. 1 (see Table I).

TABLE I

Type of Shielded and Twisted Cables for Signals up to 500 kHz (analog)

No.	Conductor size *)	No.of conductors, twisted together	Total No.of conductors per cable	1 Twist per ...mm cable length	Dimension mm outside	Cable length m	Lemosa size	Connector pin numbers
1	AWG 24	2	2	5	3.3 Ø	30	0	2
2	AWG 24	3	3	25	3.3 Ø	30	0	4
3	AWG 24	2	4	4	3.5x.38	35	1	4

*) AWG 24 $\hat{=}$ 0,25 mm^2 Cu

at ASDEX the magnetic field gradient is about $200 \cdot 10^{-4}$ Tesla per centimeter length.

In installing the cables around the experiment we took care that no closed loop appeared (high induced voltage). The opening of the loop was made on the east side of the experiment. The east half of the ASDEX can be moved 3 meters in the radial direction (to the east), and we therefore increased the cable length by this distance with a small loop in the north and south (see Fig. 3). For the equipment protection and safety system a total length of approximately 16 km cable according to Table I is installed.

Our compromise between safety requirements and cost is a hybrid of relay, solid state and computer-controlled protection systems. Relays are only used for the circuit to detect the water flow in the outlets of the toroidal field (HF), ohmic heating (OH), vertical field (V), divertor (MP) and divertor compensation (MC) coil systems. Solid state circuits are used for voltage and current

symmetry measurements, leakage currents and for some temperature measurements with Pt-100 (RTD; thermoresistance of platinum; 100 Ω at 0° C, DIN 43760, tolerance at $+100^{\circ}$C ± 0.6° K). The computer PDP 11/20, 24 kbytes, with a Neff 620 data acquisition system (128 channels, 12 bit, 50 kHz, 300 V CM voltage) is used to measure the relative motion of the coils (100 channels), strain of the structure and temperature of the ohmic heating coils (28 channels). A data logger with microprocessor technology made by Consolidated Controls (Type 90 MC1) is used as a second data acquisition system in conjunction with the PDP 11/70. This system measures 16 x 7 = 112 temperature channels. These RTD's (Pt-100) are mounted on the stainless-steel vessel on the outside surface. The ADC of the system has a conversion rate of 15 Hz, 15 bit and 300 V CM voltage. Fig. 5 shows the numbers and types of sensors which are used to make the ASDEX experiment as safe as possible. The costs for each complete channel are between DM 400,- (STATOP temperature transmitter) to DM 1.800,- (Neff System) without transducer and wiring.

2. Description of the sensor types (transducer) and electrical circuits used to detect dangerous conditions (see Fig. 5)

2.1 Temperature transducer

2.1.1 Cooling water outlet temperature. The maximum temperature rise of the coils per shot is listed in Table II.

TABLE II

Temperature Rise of the Coils per Pulse

Toroidal field coils	Ohmic heating coils	Vertical coils	Radial field coil	Divertor coils	Divertor compensation coil
40°K	15°K	$<30^{\circ}$K	$<1^{\circ}$K	51°K + $<30^{\circ}$K *	$<30^{\circ}$K
45°kA	30 kA	45 kA	2(10) kA	45 kA	45 kA

\+ part of windings, consisting of copper-berylium

* part of windings, consisting of copper

A maximum water temperature in the coils of 80°C should not be exceeded. (The baking of the vessel goes up to 150°C). During and after each shot we compare the coil temperature by measuring the temperature of the water flow inside the water outlet tube with the upper limit of the temperature transmitter. To eliminate or reduce the heat flow from the outlet tube header to the sensor, we used a special thermowell. One tube is inside the other so that the water flow almost completely surrounds the PT-100 sensor. The heat flow from the outlet tube to the sensor is almost eliminated (see Fig. 6, 7 and 8).

A RTD with a diameter of 2±0.1 mm and a sensing length of 6 mm (length of detector also 6 mm) is used[1]. Teflon cable according to Table I, No.3, is used[2].

2.1.2. Temperature measurement at the surface of the coil insulation and of the structure of the poloidal field coils. To rule out any overheating of the coils, the temperature at the surface of the insulation of each poloidal field coil is measured. As the penetration time of the heat from the copper conductor into the coil insulation is longer than the cooling time of the coil, the temperature usually undergoes only a moderate rise at the coil surface. Excess temperature would, of course, quickly result at the coil surface if the water cooling were to fail. The sensor is a RTD surface resistance temperature detector[3]. The detector is embedded in a fiber-glass silicon plate and mounted with a 0.5 mm thick stainless-steel sheet around the coils. Teflon cables according to Table I, No.2 are used[4].

For items 2.1.1 and 2.1.2 a temperature alarm transmitter with double alarm settings is used. When the temperature is below the low set point the ASDEX experiment can operate. If the temperature is above the high set point, the generators will be switched off by means of relay contacts. We used STATOP temperature alarm transmitters[5] (see Fig. 9).

I. 1) Leico Industries Inc., Casella Postale 98-20017, Rho (Milano), Italy or B. Kunze, D-8024 Oberhaching, Germany
2) Gore, D-8011 Putzbrunn, Germany
3) Heraeus Typ 1, PT-100 FKG 3/10, D-6450 Hanau, Germany
4) Dietz, D-800 München 90, Germany
5) IMT Meßtechnik, D-5300 Bad Godesberg, (Current 2 mA, range 0 to 250° C, type 3 SG

Very often the question arises about the height of the output signals of thermoelements and RTD's. In the following table the differences are listed:

TABLE III

Comparison between thermoelement and RTD signals

	passive	active
temperature transducer	thermoelement	platinum thermoresistor Pt-100 (RTD)
outside diameter	≥ 0,25 mm	≥ 2 mm
temperature range	≤2200 °C	≤ 800°C
cable	special compensating cable necessary	3(4) conductor cable (twisted) AWG 24≙0,25mm² Cu
necessary:	reference junction	1÷10 mA power supply *)
maximum output signal ($\Delta\delta$=100°K)	40 µV/K×100 K = 4 mV	general: +100°C:R=138,5 ohm 0°C:R=100.0 ohm 1) J = 1 mA: U=J×ΔR=1 mA× 38,5 ohm=38,5mV 2) J = 10 mA U=J×ΔR=10 mA× 38,5 ohm=385 mV (avoid self heating)

The RTD signal is a factor of 10 (100) greater than the thermoelement output signal. We use for the measurements an RTD current of 2,5 mA.

*) depending on RTD size, mounting and self heating

3. Pressure (water flow) transducer (flow element)

3.1 Flow measurement in cooling water outlet tubes

As flow element we used a Venturi tube made in our workshop (see Fig. 10 and 11). The cooling water velocity goes up to 6 meters per sec. (NW 16). The Venturi flow element is connected to a pressure transmitter by two 2 to 4 meter long copper tubes 6 mm in diameter. The stray magnetic field at the pressure transmitter should be smaller than 0.2 tesla. This calls for a certain distance between the transmitter and machine otherwise the upper or lower set point is decalibrated. We used the Fischer[5.1)] pressure transmitter type DG special, with microswitches and analog reading, maximum pressure 40 bar, differential pressure setting from 0 to 600 mbar. The microswitch of the upper set point is connected with a shielded cable to a relay-operated 24 V DC circuit. The logic of the relay circuit makes a sum signal of the microswitches from one toroidal field coil system (6 pressure transmitters). This sum signal is further used in the interlock chain of the machine control circuit (see Fig. 9).

4. Displacement transducer

4.1 Measurement of the relative motion between the structure and coils

As sensor for the relative motion (in our case in the mm range) between the coil system or coils and the structure we bought linear potentiometers[6)] and used cables (see Table I, No.2).

Resistance	1 kΩ
Resistance tolerance	10 %
Linear tolerance	2 %
Power dissipation (40°C)	0.2 W
Temperature range	-40°C to + 80°C (130°C)
Mech. stroke length	∼10 mm

I. 5.1) Klaus Fischer, Meß- und Regeltechnik, Bielefelderstraße 37A, D-4902 Bad Salzuffeln, West Germany

6) Megatron D-8011 Putzbrunn, Germany, Type MM 10 (80°C); Type FM 10 (130°C)

Tracks	conductive plastic
Resolution	infinite (in practice 50 µm)
Permeability	<1.03
Size of the potentiometer body	7.2 x 8.2 x 32 mm
Life time	1 x 10^6 cycles

The above-mentioned potentiometer with a beryllium copper spring is built in a brass tube, as shown in Fig. 13, 14 und 15. A Teflon cable (see Table I, No.2) is used to complete the bridge circuit in the control room. The bridge completion resistor is a 10 kΩ potentiometer. With this potentiometer it is possible to make the zero adjustment (see Fig. 12). The bridge calibration is done with a micrometer by changing the bridge voltage. The sensitivity of the bridge is usually 1 V per mm at a bridge voltage of U_B = 10 V (10 mA) for a gain of 1. Fig. 16 shows a flange of the vacuum vessel and two linear potentiometer mounted to measure in a high vacuum system the displacement of the getter panel in the φ- and ρ-directions (see Fig.39 for notation). Fig. 17 and 18 show a photograph and the design of a linear potentiometer mounted on an aluminium bar 30 x 30 mm to measure the radial displacement of the inner ohmic heating coils.

N.B.
In an environment of high temperature, high vacuum, neutron flux and x-ray bombardment a capacitive displacement transducer could be used.

5. Force and displacement transducer realized with strain gauges

5.1 Measurement with strain gauges

For the weight alignment of the stainless-steel vessel we bought 8 pressure transducers[7] with a range from 0 to 200 kN (kilonewton). The weight of the complete vessel is 200 kN to 400 kN (depending on the kind of diagnostics applied). With this pressure transducer (height 20 mm) we measure the weight distribution of the vessel at 8 points around the torus with resistance strain gauges. Two gauges are arranged to pick up

I. 7) Erichsen, D-5600 Wuppertal, Germany

the positive longitudinal strain and two gauges the negative transverse (Poisson) strain, forming a complete bridge circuit (linear). Each pressure transducer has 3 such complete Wheatstone bridges connected in series.

Transducer output	2 mV at 200 kN (U_B = 1.0 V)
Transducer output	4500 µm at 200 kN (k = 1.9; U_B = 1.5 V)
Ohmic resistance	360 Ohm
Type	731 -20
Outside diameter	120 mm
Inside diameter	80 mm
Height	20 mm
Temperature range	20°C to 120°C
Permeability	1.01
Range	0 to 200 kN
Tolerance	1%
Strain gauge type	WK 09-030-WT-120 (Vishay)
Ohmic resistance	120 Ohm

The pressure transducer is connected with a Teflon cable (see Table I, No.3) to the control room. The cable shield is on the pressure transducer floating. For measurement we used the strain gauge bridge type P 350 A supplied by Vishay. It is important to measure the output signal of each transducer before it is mounted. The output signal should then be zero. A photograph of the transducer is seen in Fig. 19.

5.2 Strain gauges arranged in a Wheatstone bridge configuration to measure small displacements (<50 µm)

The resolution of the linear potentiometer (see Sec.4) below 50 µm is not good enough for display because of the rough surface of the conductive plastic material.

A different way to measure small displacements in a magnetic field environment (see Fig. 19a) is to use strain gauges (resistance changes), e.g. Type WK-09-125 WJ-700 (Vishay, D-8032 Lochham/Munich) with the following features:

1) glass-fiber-reinforced epoxy-phenolic resin-backed gauges
2) nickel chromium foil (Karma); small magneto-resistance
3) zero shift: ε = + 5 µm/m after 30 days /7/
   ε = + 45 µm/m after 900 days
4) maximum strain $\varepsilon = \pm 1000$ µm/m
5) temperature range - 268÷ + 275°C
6) magnetic field compensation by reducing the wiring loop area as far as possible /8/; /9/

   6.1) the above-mentioned strain gauge consists of an active gauge surmounted by a passive gauge bifilarly connected to cancel adjacent loops

   6.2) internal Wheatstone bridge wiring done with printed circuit or

   6.3) to reduce the induced voltage in the wire cable, a method of twisting Kapton-insulated wire with very tight turns (more than 6 turns per cm cable length) has been developed.

   6.4) reduce magnetic field by Mu metal shielding. The first (outside) layer should be steel alloy with a saturation limit of 2,5 tesla (initial permeability of μ_o = 300). A Cu shield should be followed by a Mu metal layer. Saturation limit 0,8 tesla (initial permeability μ_o = 25000)

7) temperature compensation for stainless steel
8) internal resistance of each gauge 2 x 350 ohm = 700 ohm
9) k-factor of 2
10) thermovoltages; D.C. and A.C.-fed systems are discussed in /10/
11) The cable (2 pairs) should be symmetrically twisted (at least 2 turns per cm cable length) (conductor size AWG 24 or 26). The capacitance difference between the 1st conductor and braid and 2. conductor and braid should be less than 2%. All conductors in the cable should come from the same copper charge (same resistance per unit length).

Item 6.4 was not applied in our case because the toroidal magnetic field at the location of the strain gauge was ~6 tesla.

U_M	V	output voltage
U_B	V	supply voltage
k	1	gauge factor
ε	1	mechanical strain
σ	$\frac{N}{mm^2}$	stress
E	$\frac{N}{mm^2}$	modulus of elasticity
F	N	force
M	Nm	bending moment
ℓ	m	length
J	m^4	moment of inertia of area
W	m^3	resisting moment
h	m	height
b	m	width
f	m	deflection

Sensitivity calculation of the Wheatstone arrangement according to Fig. 19a

ℓ = 110 mm
h = 2 mm stainless steel
E = $21 \cdot 10^6$ N/mm^2
k = 2
U_B = 1 V

We used a differential amplifier with gain = 10^5 and measured in a frequency range between D.C. and 1 kHz.

Sketch 1
Wheatstone bridge

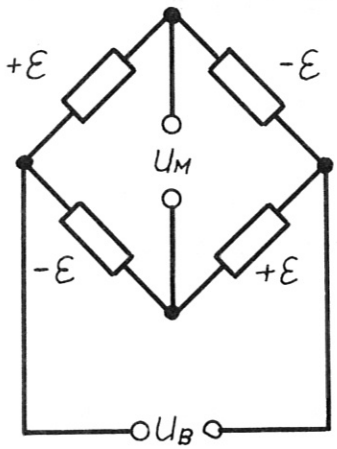

Sketch 2

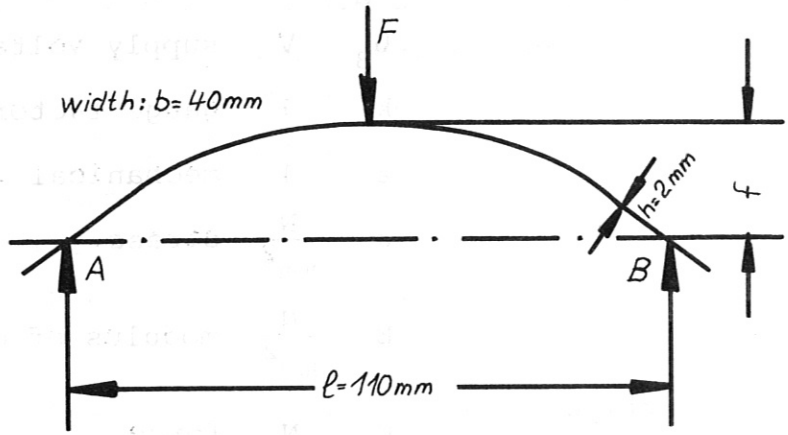

$$\frac{U_M\,[mV]}{U_B\,[V]} = k[1]\cdot\varepsilon\left[\frac{\mu m}{m}\right]\cdot 10^{-3}$$

or general (see sketch 1):

$$\frac{U_M\,[V]}{U_B\,[V]} = k[1]\cdot\varepsilon\left[\frac{m}{m}\right]$$

Hooke's law:

$$\sigma = E\cdot\varepsilon$$

bending moment:

$$M = \frac{F\cdot\ell}{4}$$

moment of inertia of area:

$$J = \frac{b\cdot h^3}{12}$$

stress:

$$\sigma = \frac{M}{W} = \frac{M}{J}\frac{h}{2} = \frac{F\cdot\ell}{4}\cdot\frac{12}{b\cdot h^3}\cdot\frac{h}{2} = \frac{F\cdot\ell\cdot 3}{2\cdot b\cdot h^2}$$

deflection (see sketch):

$$f = \frac{F\cdot\ell^3}{48\cdot E\cdot J} = \frac{F\cdot\ell^3}{4\cdot E\cdot b\cdot h^3} = \sigma\frac{\ell}{6\cdot d\cdot E} = E\cdot\varepsilon\cdot\frac{\ell^2}{6\cdot d\cdot E} = \varepsilon\frac{\ell^2}{6\cdot d} = \frac{U_M}{U_B\cdot k}\frac{\ell^2}{6\cdot d}$$

$$f = \frac{U_M}{U_B\cdot k}\cdot\frac{\ell^2}{6\cdot d}$$

$$\frac{f}{U_M}\left[\frac{mm}{V}\right] = \frac{\ell^2}{U_B\cdot k\cdot 6\cdot d} = \frac{110^2}{1\cdot 2\cdot 6\cdot 2} = 504\left[\frac{mm}{V}\right];\ \text{gain}=1$$

$$\frac{f}{U_M}\left[\frac{\mu m}{mV}\right] = 504\left[\frac{\mu m}{mV}\right];\ \text{gain}=1$$

$$\frac{f}{U_M}\left[\frac{\mu m}{V}\right] = 5.04\left[\frac{\mu m}{V}\right];\ \text{gain}=10^5$$

Protection of electrostatic shielding is achieved by surrounding the cable and the bridge with a metallic layer. This may be either braid or aluminium foil or both. Braid with high optical coverage will provide more protection. To lower this interference (EMC) further the Wheatstone bridge should be operated with a constant current power supply, which means $R_{i \text{ power supply}} \rightarrow \infty$.

Therefore the voltage induced in the still existing small wiring loops can only drive a very small noisy current because of the high resistance of the whole circuit.

6) Coil protection by voltage symmetry

To protect the 16 toroidal field coils against short-circuiting and earth connection resulting in very high asymmetrical forces, we compare the analog voltage drop of coil pairs in opposite directions e.g. of coil 1 with the voltage drop in coil 9, coil 2 with coil 10 etc. (see Fig.20). Because of the coil symmetry the voltage drop (inductive and ohmic parts of the voltage drops) under normal conditions is the same in each coil; this means we can easily compare the differential voltage divider (see Fig. 21 and 25) for coil 1 and coil 9 should have a tolerance of only 0.1%. This is achieved by selecting the 100 kΩ and also the 100 Ω resistors[8] for the voltage divider. All voltage dividers are tested with 20 kV (rise time 20 µs). The differential voltage divider is connected to ground and also the cable grid at the same point. A Teflon cable according to Table I, No. 2 is used. When the voltage drop in one coil reaches the upper set point, the level discriminator (see Fig. 22) is the activated (1600 V/16 coils = 100 V; 100 V x 10/1000 = 1000 mV). 1000mV is the upper set point. When the voltage difference between coil 1 and coil 9 reaches a certain value, in our case 20 V (20 V x 10/1000 = 200 mV), the dual comparator (see Fig. 23) closes a relay contact and the 1.45 GJ generator will be switched off. The frequency response of the system is 100 kHz. Because of the alternating voltage component from the rectifier with a frequency of 300 Hz we reduced the speed of the measurement system to 170 Hz.

I. 8) Power resistors
a) 100 kΩ±1%; 25 W, Type HVR 30 D; MBS(CGS, Lymington, Hampshire), D-8000 München 44, West-Germany
b) 100 Ω±0.1%; 4 W; Type MS245 N (non-inductive) Caddock Wetronik, D-8000 München 80, West-Germany

A similar voltage-symmetry protection system is used for the upper and lower parts of OH coils, MC coils, MP coils and V coils. The measurement system can be automatically tested before each shot (see Fig. 24, 26 and 27). To conduct these tests, one needs a time of about 2 minutes. Only the high-voltage resistor cannot be tested.

The above mentioned protection system is very important for the safety of the poloidal and toroidal field coils. These coils have a relative low time constant and in the case of a failure caused by arcing or a short circuit in one of the coil systems the fault condition will be detected. In this case the main power supply of the individual coil system will be switched off.

7. Coil protection by current symmetry

To reduce the magnetic forces acting on the current leads of the divertor coils it was necessary to avoid bifilar leads and to apply triple leads with more symmetric current distribution. In this case the j x B force is reduced, (J = current distribution in the divertor coil lead; B = induction of the toroidal field.)

To detect the current splitting we compare the currents in the upper and lower current leads (up to 22,5 kA) between the inner (1), middle (2) and outer (3) divertor coils (see Fig.2 for numbering and Fig.28).

As seen from Fig.28 the positive D.C. current is divided in two high current leads so that the current is only 50% in each lead and therefore the above mentioned force is reduced.

This current distribution of 50% is measured in the upper and lower coil triplets and the current difference should be smaller then 5%. With a Rogowski coil (see Fig. 33) we measure the upper and lower lead current and compare the output voltages of two active integrators (level discriminator) /11/ (see Fig. 30) in one dual comparator (see Fig. 29). When the signal of the current difference is greater than 5% we make an emergency stop.

A photograph of the test and control units mounted in a NIM crate is shown in Fig. 31.

8. Rogowski coil

Rogowski coils (see Fig. 32, 33, 34) are used to measure

$$e = \frac{d\phi}{dt} = A \times N \times \frac{dB}{dt} \; [V]$$

where

e	[V]	induced coil voltage	B	[T]	magnitude of the magnetic induction inside the coil
ϕ	[Vs]	magnetic flux	J	[A]	current to be measured
t	[s]	time	μ_o	$\left[\frac{Vs}{Am}\right]$	$4 \times \pi \times 10^{-7}$ permeability
A	[m^2]	coil area	r	[m]	radius of field lines of the coil
N	[turns]	number of turns	dℓ	[m]	length of flux line

Biot-Savart Law

If the current distribution is high enough to permit easy evaluation of the line integral $\oint B \times d\ell$ the Rogowski coil, it is then

$$\oint B \cdot d\ell = \mu_o \cdot J \cdot N$$

$$(B)(2 \cdot \pi \cdot r) = \mu_o \cdot J \cdot N$$

$$B = \frac{\mu_o \cdot J \cdot N}{2 \cdot \pi \cdot r}$$

$$e = \frac{d\phi}{dt} = A \frac{dB}{dt}$$

Sketch 3

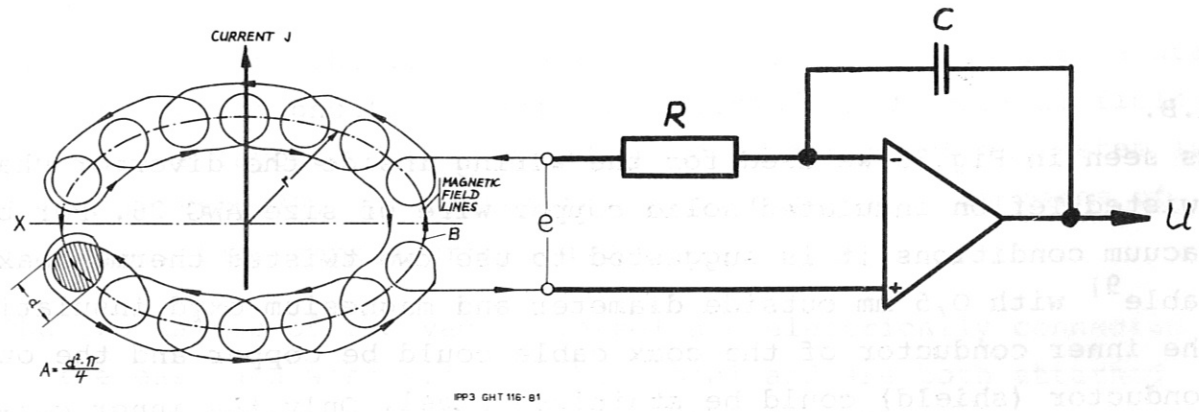

Rogowski coil

active integrator

$$U = \frac{\mu_o \cdot A \cdot N}{2 \cdot \pi \cdot r} \cdot \frac{1}{J} \cdot J$$

We design the Rogowski coil (number of turns N; area of each winding A) in such a way that the time constant $\tau = R \cdot C$ in the active integrator is ≥ 10 ms and the output signal of the active integrator $U \geq 1$ V at the nominal current J.

The Rogowski coil for symmetrical current measurement (see Fig. 33 and sec. 7) has 2 layers of windings and N = 1120 turns, an area of A = 78 mm^2 and a polyimide (Vespel) coil body.

The Rogowski coil winding is not wound completely around the high-current lead because of stray fields transverse to the coil. The winding gap is denoted in sketch 3 by X.

Fig. 34 shows a Rogowski coil mounted inside an ultrahigh vacuum ($< 10^{-8}$ mbar) in the divertor chamber of the ASDEX vacuum vessel. For outgassing reasons we used a special design which looks like a winding network. The electric current in the N_2-pipe should be zero during the plasma experiments. Only in the case of ground loops will there be a current, which should be detected.

9. Magnetic probes

To reduce dangerous eddy currents induced by plasma disruptions, the 26 getter panels are made of anodized aluminium profiles. By measuring $\frac{d\Phi}{dt}$ near the getter panels with a magnetic probe /12/ we can calculate the value of the eddy current (see Fig. 35). The output of the active integrator signal is proportional to the magnetic field near the getter panel (see Fig. 36).

N.B.
As seen in Fig.35 we used for the wiring inside the divertor chamber twisted Teflon insulated solid copper wire of size AWG 26. For better vacuum conditions it is suggested to use two twisted thermo-coax cable[9] with 0,5 mm outside diameter and magnesium oxyd insulation. The inner conductor of the coax cable could be copper and the outside conductor (shield) could be stainless steel. Only the inner conductors are connected to the magnetic probe.

9) Thermo coax cable, Philips, D-3500 Kassel, West Germany

10. Active integrators

In our case a fast active integrator is used to solve analytically the following equations:

current: $i = \frac{1}{M}\int U \cdot dt \; [A]$ M = mutual inductance $[H]$

induction: $B = \frac{1}{A}\int U \cdot dt \; [T]$ A = coil area $[m^2]$

The general equation of an active integrator is

$$U = \frac{1}{\tau}\int e \cdot dt \; [V] \qquad \tau = \text{time constant} \; [s]$$

Sketch 4

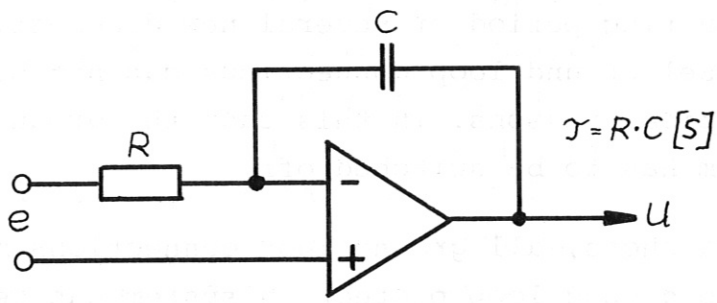

The output signal U should be of the order of 1 V and the time constant if possible greater than or equal to 10 ms. Therefore, we choose R = 10 kΩ; C = 1 µF. The layout of an active integrator is seen in Fig. 37 and the photograph in Fig. 38.
An active integrator with a fast operation amplifier, a drift compensation amplifier and an offset amplifier is discussed in /13/.

11. Ground loop protection

Ground loops on the vacuum vessel are very dangerous for feedback systems and diagnostic systems and poloidal and toroidal field coils. The layout of the ground connection protection system is shown in Fig. 39. The vessel is electrically slit by means of two insulation gaps (north and south).

The two halves of the vacuum vessel are electrically connected on the east and west side of the vessel and are both attached to a $R_1 = 4\,\Omega$ Morganite power resistor to earth.

This is done to reduce as far as possible any dangerous voltage being applied to the vacuum vessel in the event of electrical failure during the plasma pulse. After the plasma shot the ground detection system is switched on and each resistor (ground connection) parallel to R_1 which is smaller than 1 kΩ will be detected. After detection a horn will sound in the control room and experimental area, and the ground connection then has to be found. For safety reasons we disconnect automatically the ground loop measurement system from the vacuum vessel grounding system during the plasma pulse.

11.1 Method to locate ground loop connections

During the mounting period of several new diagnostic systems at the ASDEX vessel ground loop connections can not be avoided because of practical reasons. In this case the ground loop protection system has to be switched off.

Between plasma shots, all ground loop connections must be located before the ground loop protection system can be activated again.

This can be done as follows:
A 10 kHz, 50 W audio frequency generator[10] Typ FLS10/50 is used to couple the frequency with a current transformer[10] to the ASDEX vessel near the Morganite resistor R_1 (see Fig. 39). The 10 kHz current from the vessel to the ground can now be detected by a flexible Rogowski coil of approximately 1,5 m length (~50 cm in a diameter) and an oscillograph.

I. 10) SEBA-Dynatronic, D-8601 Baunach, West Germany

12. Data acquisition system

12.1 Introduction

The Neff system is a complete data acquisition system that converts low-level analog input signals (mV) to digital form by means of a digital computer (PDP 11/20) (see Fig.40). The system provides the required signal conditioning, amplification, filtering and multiplexing for 128 (12 bits) channels at rates of 50 kHz (2.6 ms per channel). The preamplifier has a CMR of 300 V DC or 400 V AC peak without damage (see Fig. 42).

12.2 Signal conditioning

A signal conditioning subsystem provides all input conditioning required for resistance temperature devices (RTD), in our case PT-100 (100 Ω at $0^{\circ}C$); linear potentiometers (1 kΩ) and strain gauges (see Fig. 41). It features programmable calibration and shares the computer interface with the analog signal processor. Each channel is configured for a particular type of transducer by a plug-in mode card. A regulated power supply for each channel supplies either constant voltage or constant current excitation with remote sensing in constant-voltage mode. Input calibration is performed under control with the standard system providing both zero and upscale calibration points for each type of transducer.

The channel numbers, gains, channel abbreviations, maximum and minimum set points and the gauge factor are coded in a MACRO program section and may be changed in real-time by the operator. The list is printed on the LA-36 as seen in Fig.43 for real-time control. After the plasma shot it is possible to get also the plot data display from the computer PDP 11/70 (see Fig.44).

12.3 Software

The purpose of this supervisor computer is to measure repeatedly all the 128 analog inputs and to compare the measured values with two tables containing the maximal and minimal allowed values. If any value exceeds one of the limits, an alarm bit in an output register will be set, activating a relay which causes an audible alarm and an action according to chapter 13 (pulse stop or emergency stop).

In order to ensure the proper operation of the supervisor system, the program sets another output pulse after each conversion cycle. This signal is connected to a watchdog timer. If the computer stops or the program is aborted by any reason, the watchdog timer sets another alarm condition after a few milliseconds and the action of the emergency switch will be similar.

It is important to minimize the time between the occurence of a dangerous condition in the experiment and the activating of the emergency stop by the computer. Therefore, the computer program has been optimized in the following manner. There are two tables, each of which is normally 128 words long: one with the channel number and the corresponding gain setting in each word and the other with the converted values corredponding to the channels indicated by the first table. The first table is sent by a direct memory access (DMA) device to the A/D converters. The computer can start the transmission of the table by a single operation, all other is done by hardware. Another DMA device is synchronized with the first one and puts the measured values into the second table. There are two samples of the second table containing the measured values. When one conversion cycle is finished, the program starts immediately a new cycle with the other sample of the second table and has now time to compare the contents

of the non-busy table with the tables containing upper and lower limits.

The interleaved operation allows to check all channels each 3 milliseconds. Because it is not necessary to place the channels in any order into the first table, one can shorten it to get shorter cycle times.

There are two ways of editing channel numbers, channel abbreviations, maximum and minimum set points and the gauge factors. They can be coded in a convenient way in a MACRO program section and are therefore available when the system is loaded into the computer, or they may be altered at run time at the console terminal. The second method is useful for making little modifications such as setting single channels offline or changing limits. For channels with no stable bias one can switch to "relative limits". In this case the values of the last measured bias (measured in a special program mode when the experiment is not active) are added to the limits. A typical printout of the settings on the console terminal (LA36) is shown in Fig. 43.

In an additional operating mode the measured values can be sent to the host computer (PDP 11/70) during the shot in suitable time intervals (e.g. each 200 ms) and may be plotted there (see Fig. 44).

13. Actions taken on reaching the individual set points

Before or during the plasma pulse different actions are taken, depending on the kind of transducer signals which are reaching the upper or lower set points (see Table IV):

TABLE IV

On Reaching the Lower or Upper Set Point Limits Between or During the Plasma Pulse

At reaching the lower or upper set point at:	Following actions are taken	
	Before the pulse	During the pulse
Temperature	stop next pulse	stop next pulse
Flow	stop next pulse	stop next pulse
Displacement	pulse stop	emergency stop
Voltage symmetry	pulse stop	emergency stop
Current symmetry	pulse stop	emergency stop

Acknowledgements

We wish to thank J. Finkelmeyer, J. Franzspeck, F. Gresser, F. Hartz, W. Jakobus, G. Klement, P. Krüger, M. Kornherr, H. Kotzlowsky, N. Niedermeyer, M. Pillsticker, H. Rapp, H. Wedler, F. Werner, F. Wesner for many helpful discussions and advice. Thanks are also due to K. Sahner and H.J. Berger and our workshop for construction, mounting and cable-laying work involving several kilometers of cable from the experiment to the control room. The authors wish to thank T.Henningsen for his preparation of the photographs.

I. NOTE:

Reference to a company-product or name does not imply approval or recommendation of the product by IPP to the exclusion of others that may be suitable.

References

/1/ GERNHARDT,J. et al., FUSION TECHNOLOGY 198o, Vol.1, p.641-647
An Equipment Protection and Safety System for ASDEX Tokamak

/2/ THE ASDEX GROUP, IPP-Report III/47 (1978)

/3/ RAPP,H. et al, FUSION TECHNOLOGY 198o, Vol.2, p.9o3-9o8
The ASDEX Overvoltage Protection System

/4/ WEDLER,H. et al., FUSION TECHNOLOGY 1978, Vol.1, Page 43 to 48,
Testing and Performance of the 3O kA Ohmic heating system for ASDEX

/5/ PILLSTICKER,M. et al., FUSION TECHNOLOGY 198o, Vol.1, p.461-466
Operational Test and Final Technical Concept of the ASDEX Multipole Magnetic Field Coils

/6/ GERNHARDT,J. et al., IPP-Report (under preparation) III/67, 1981
Low noise cable for diagnostic, control and instrumentation for ASDEX

/7/ FREYNIK Jr.,H.S. and DITTBENNER, G.R., Lawrence Livermore Laboratory CA 9455O
Strain-Gage-Stability Measurements for Years at 75°C in Air
(VISHAY D-8O32 Lochham/Munich)

/8/ TELINDE, J.C., Strain gage instrumentation for magnetic driven flyer plate facility. Mc-Donnell Douglas Astronautics Company (VISHAY, D-8O32 Locham/Munich)

/9/ HARTWIG, G. WUCHNER, F., Tieftemperatureigenschaften von Dehnungsmeßstreifen (7 Tesla), Institut für Experimentelle Kernphysik III, Karlsruhe, (VISHAY; D-8O32 Locham/Munich)

/1O/ STEIN,P.K. (Phoenix Arizona), Information conversion as a "NOISE"-suppression method (VISHAY, D-8O32 Locham/Munich)
Lf/MSE Publication No.66

References (cont.)

/11/ GERNHARDT,J. et al., IPP Report III/15 (1974)
Method to measure very high D.C. currents with active integrators (in German)

/12/ GERNHARDT,J. et al., IPP Report III/59 (1980)
Design of Magnetic Probes for MHD Measurements in ASDEX Tokamak

/13/ GROENING,D.E., IPP Report III/63 (1980)
Optimization of active integrators (in German)

Figure captions

Fig. 1: The two completed halves of ASDEX

Fig. 2: Upper cross section of ASDEX

Fig. 3: Numbers and types of transducers and transmitters used

Fig. 4: Cable path in the ASDEX experiment

Fig. 5: Cable ducts located in the basement

Fig. 6: RTD (Pt-100) mounted near the cooling water outlet header

Fig. 7: Photograph of RTD

Fig. 8: Photograph of RTD and flow element

Fig. 9: Control racks located in the basement

Fig.10: Venturi flow element

Fig.11: Photograph of Venturi flow element

Fig.12: Bridges for displacement measurement

Fig.13: Linear potentiometer to measure displacements from 50 µm to 10 mm

Fig.14: Photograph of linear potentiometer

Fig.15: Linear potentiometer for inner vertical and divertor compensation coils and surface RTD for radial field

Fig.16: Photograph of two linear potentiometers to measure the displacement (<10 mm) in the φ - and ρ-directions of the getter panel

Fig.17: Photograph of displacement measurement at the inner ohmic heating coil

Fig.18: Linear potentiometer arrangement to measure displacement on the inner ohmic heating coils

Fig.19: Pressure transducers to measure the weight distribution

Fig.19a: Strain gauge arranged in a Wheatstone bridge to measure displacement (strain) on high current-leads

Fig.20: Voltage symmetry measurement of the 16 main field coils

Fig.21: Differential voltage divider; 0,1% tolerance

Fig.22: Level discriminator for maximum measurement (symmetrical voltage)

Fig.23: Dual comparator for symmetrical measurement (voltage)

Fig.24: Self test assembly (symmetrical voltage)

Fig.25: Photograph of differential voltage divider mounted at the outside of the main field coil

Fig.26: Self test unit, discriminators and comparators mounted in a NIM crate (symmetrical voltage)

Fig.27: Test voltage for self test assembly (symmetrical voltage)

Fig.28: Current symmetry of upper and lower divertor coils

Fig.29: Dual comparator for symmetrical measurement (current)

Fig.30: Integrator, level discriminator for maximum measurement (symmetrical current)

Fig.31: Photograph of test unit and control unit mounted in a NIM crate (symmetrical current)

Fig.32: Rogowski coil for current measurement

Fig.33: Rogowski coil for divertor coil mounted on the busbars for current measurement

Fig.34: Rogowski coil for electric N_2 pipe mounted in the divertor chamber

Fig.35: Magnetic probe to measure $\frac{dB\delta}{dt}$ inside the divertor chamber

Fig.36: Electrical circuit of magnetic probe

Fig.37: Highly stable active integrator (differential)

Fig.38: Photograph of active integrator mounted on EUROPA crate

Fig.39: Measurement of ground loops at the ASDEX vacuum vessel

Fig.40: Photograph of real-time computer (PDP 11/20) and data acquisition system mounted in a rack

Fig.41: Photograph of printed circuit of input for conditioner unit

Fig.42: ASDEX data acquisition system (Neff, 620-100/300), 50 kHz, 12 bit, 128 channels, 300 Volt common mode voltage

Fig.43: List of channel numbers, upper and lower set point limits, offset, gain and gauge factors for real time data acquisition system

Fig.44: Plot data of displacement and temperature of each individual channel as function of time

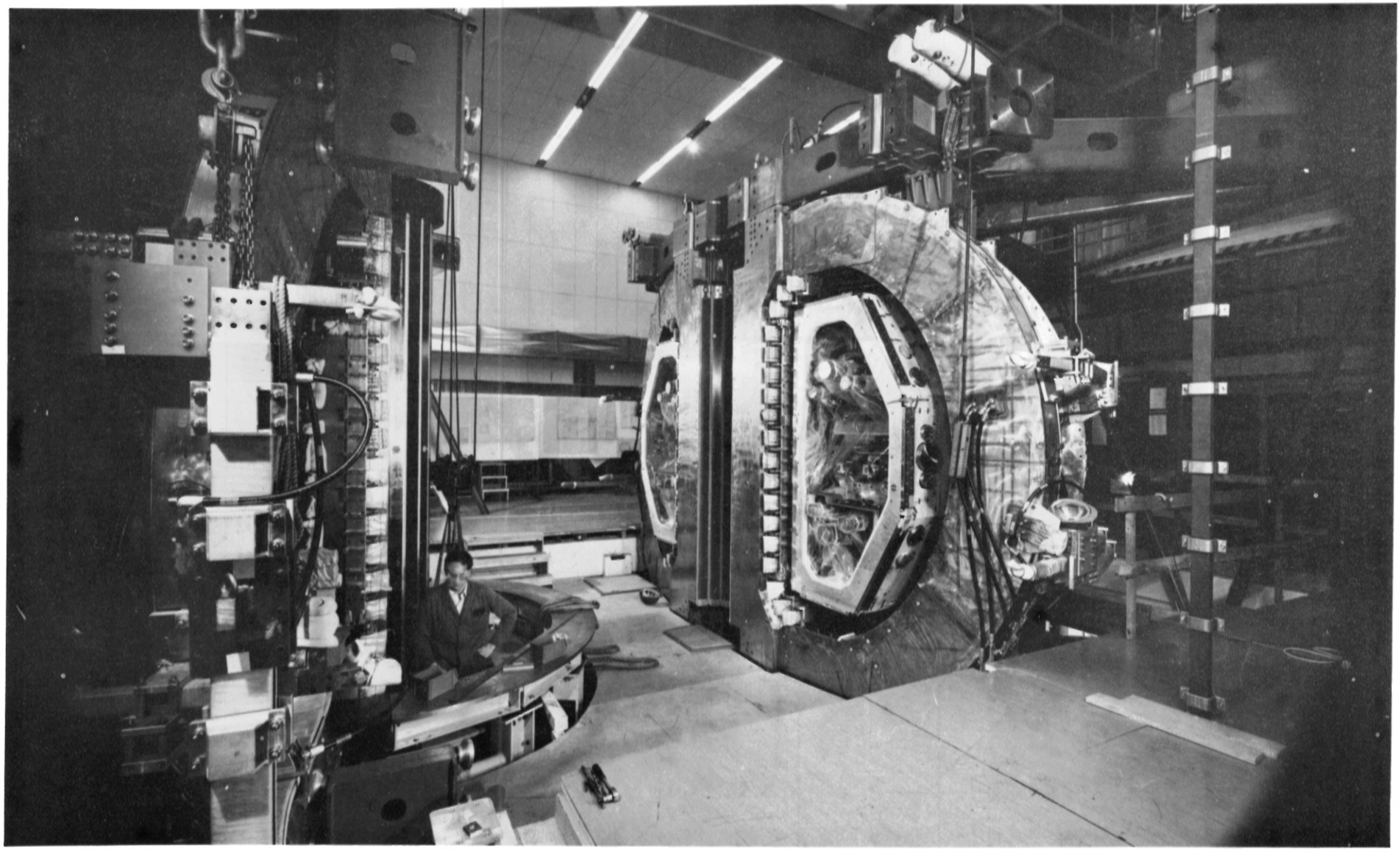

FIG.1: THE TWO COMPLETED HALVES OF ASDEX

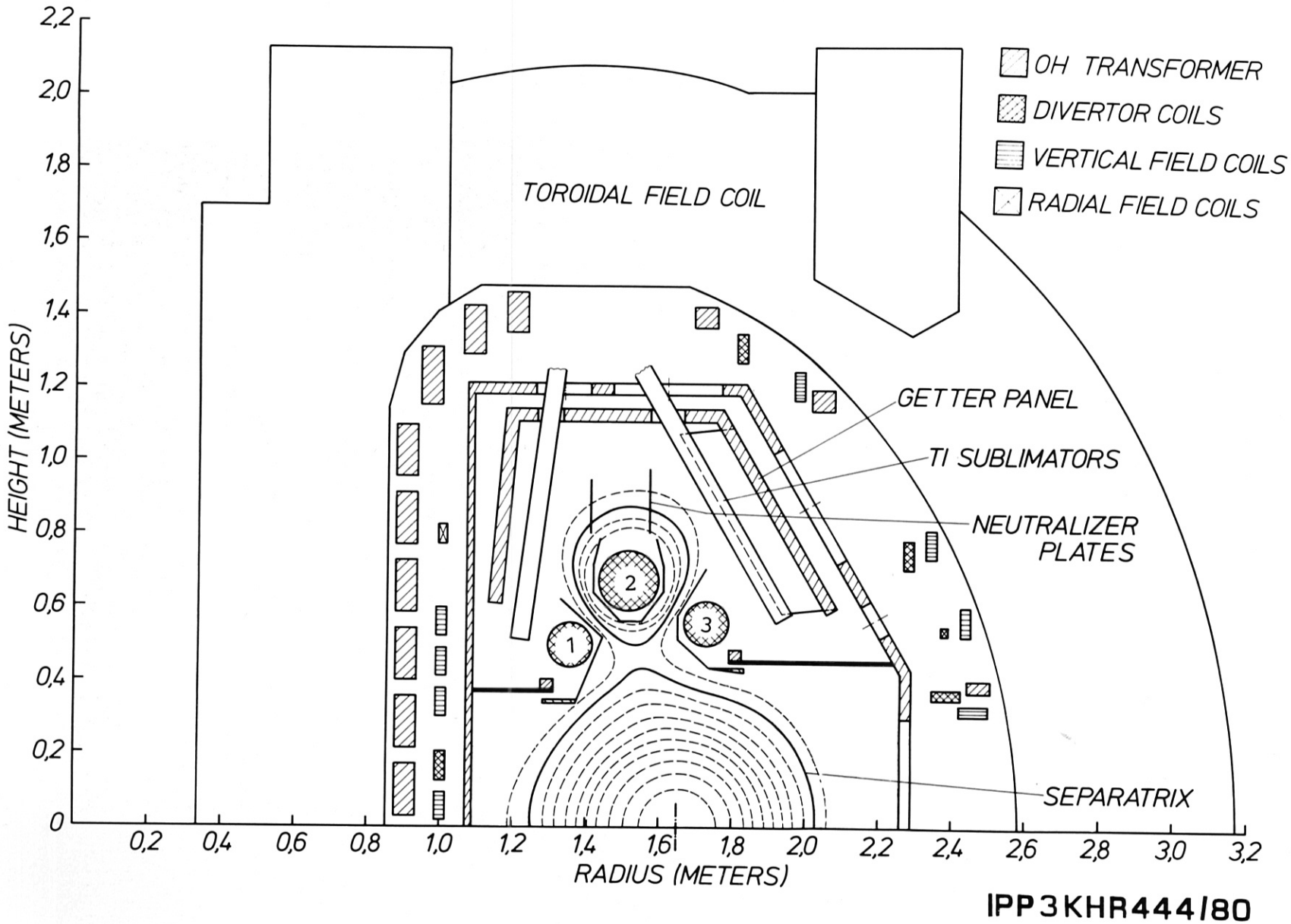

FIG. 2: UPPER CROSS SECTION OF ASDEX

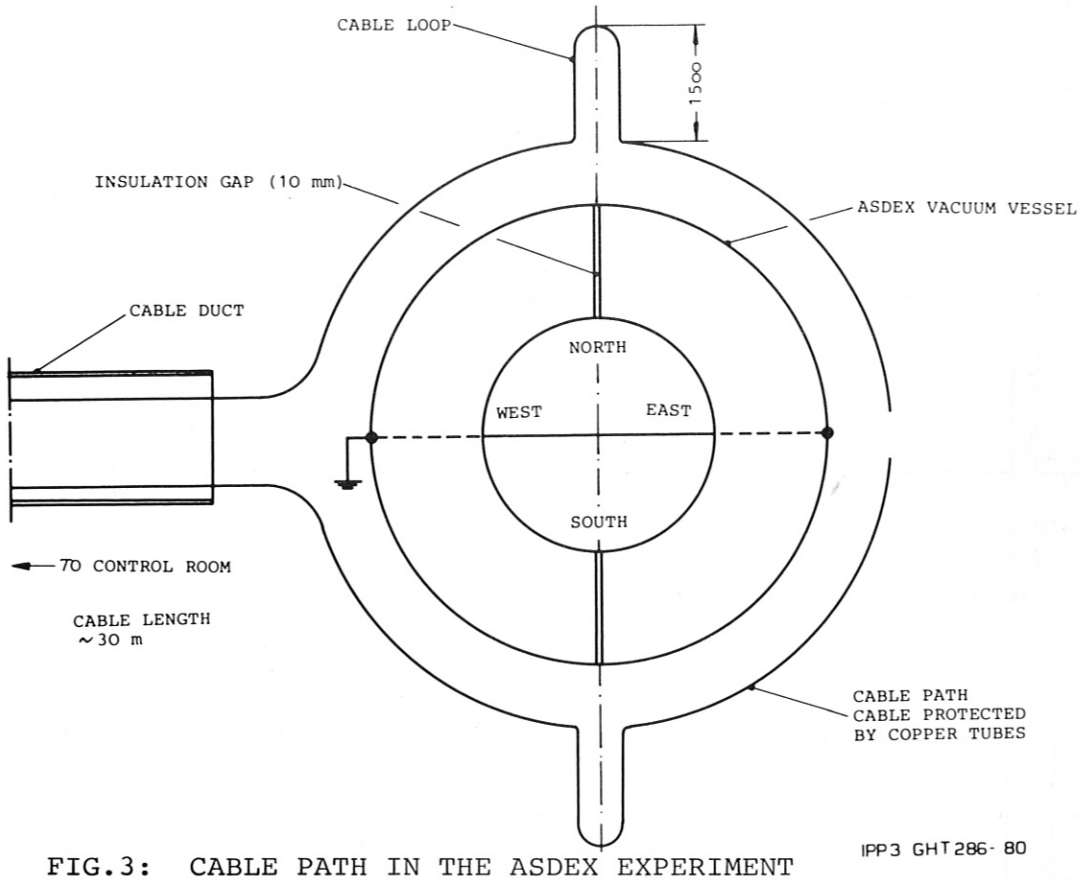

FIG.3: CABLE PATH IN THE ASDEX EXPERIMENT

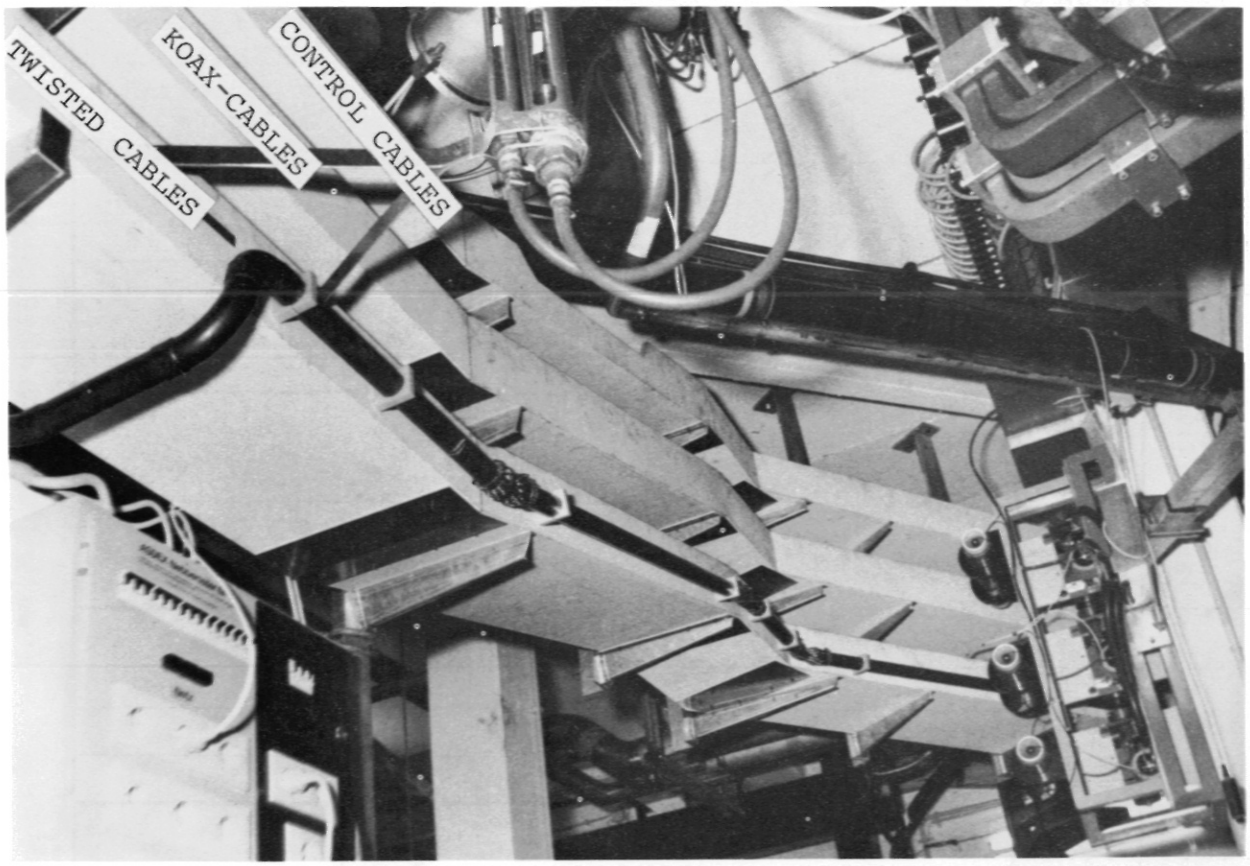

FIG. 4: CABLE DUCTS LOCATED IN THE BASEMENT

M = MOUNTED

U = USED

PARTS WHICH ARE CHECKED	TEMPERATURE			FLOW		DISPLACEMENT				WEIGHT		SYMMETRY				CURRENT	MAGN.FIELD
	TRANS-DUCER PT-100		TRANS-MITTER	TRANS-DUCER VENTURI TUBE	TRANS-MITTER	TRANS-DUCER POTENTIOM.		TRANS-MITTER	RADIAL DISPLACEM. MAX. mm	TRANS-DUCER STRAIN GAUGE	TRANS-MITTER	VOLTAGE TRANS-DUCER VOLT.DIVID.	TRANS-MITTER COMPAR.	CURRENT TRANS-DUCER ROGOWSKI COIL	TRANS-MITTER COMPAR.	ROGOWSKI COIL IPP [4]	MAGN. PROBE IPP [5]
	M	U				M	U										
CENTRAL SUPPORT COLUMN	2	1	STATOP	-	-	16	16	NEFF	0.7								
TOROIDAL FIELD COILS	3	1	STATOP	16x6=96	FISHER	48	32	NEFF	2.5			IPP	16/8				
OH COILS	14	14	STATOP	14	FISHER	36	36	NEFF	0.6			IPP	2/1				
OH COIL SUPPORT	3	3	STATOP	-	-	-	-	-	-								
OH COIL RESISTOR	6	3	STATOP	6	FISHER	-	-	-	-								
OH COIL INSULATION	18	18	STATOP	-	-	-	-	-	-								
VERTICAL FIELD COIL	3	3	STATOP	3	FISHER	12	12	NEFF	1.0			IPP	2/1				
RADIAL FIELD COIL	4	2	STATOP	-	-	-	-	-	-								
DIVERTOR COILS	14	14		8	FISHER	14	14	UV-OSC.	1.4			IPP	6/3	IPP	6/3		
DIVERTOR COMPENSATION COILS	4	4	STATOP	4	FISHER	4	4	NEFF	1.0			IPP	2/1				
STAINLESS-STEEL VESSEL	128	76	DATA-LOGGER	-	-	64	24	UV-OSC.	7.0	8	VISHAY						
PASSIVE COIL (HIGH VACUUM)	-	-	-	-	-	-	-	-	-							2	
N_2 TUBE (HIGH VACUUM)	-	-	-	-	-	-	-	-	-							1	
DIVERTOR (HIGH VACUUM)	3	3	DATA-LOGGER	-	-	2	2	OSC.									1

IPP3 GHT 338-80

FIG. 5: NUMBERS AND TYPES OF TRANSDUCERS AND TRANSMITTERS USED

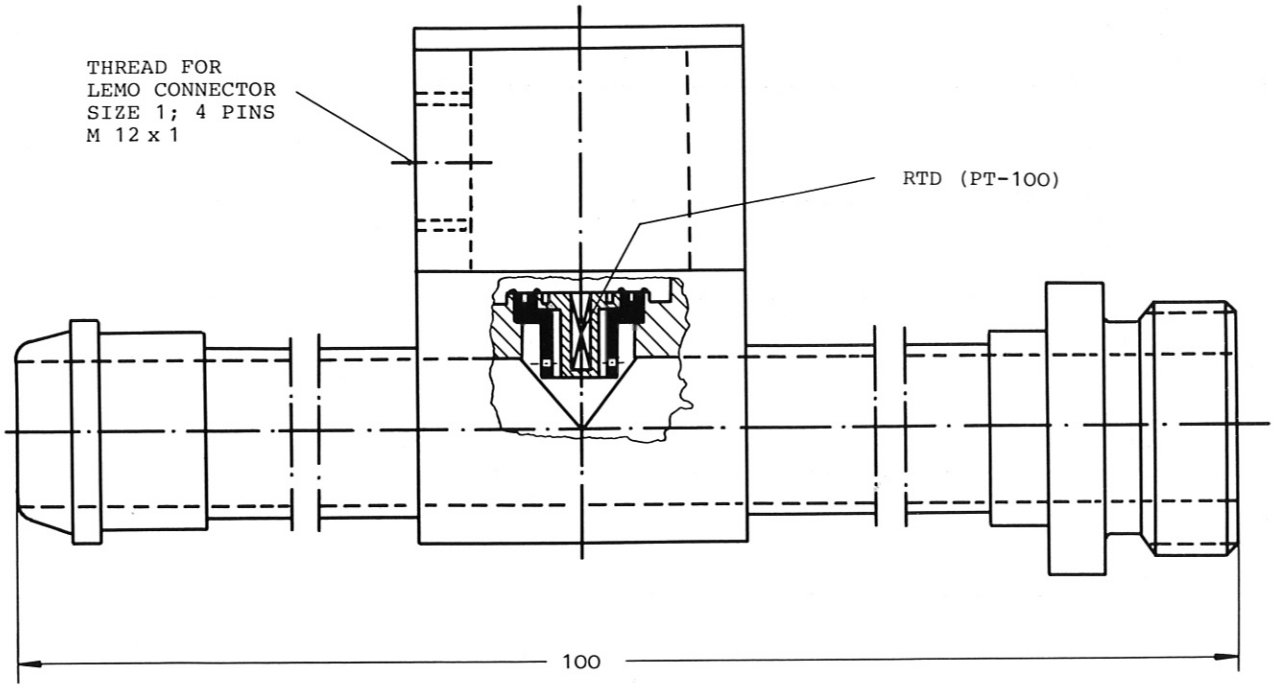

FIG. 6: RTD (PT-100) MOUNTED NEAR THE COOLING WATER OUTLET HEADER

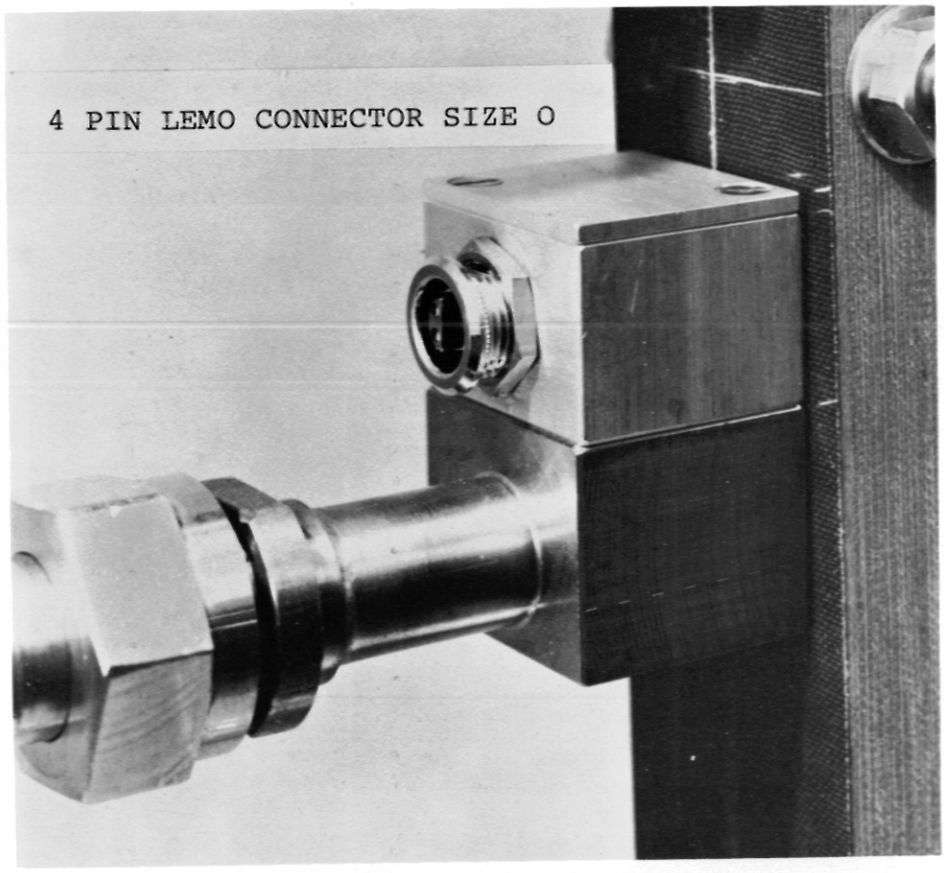

FIG. 7: PHOTOGRAPH OF RTD (FOR DESIGN SEE FIG. 6)

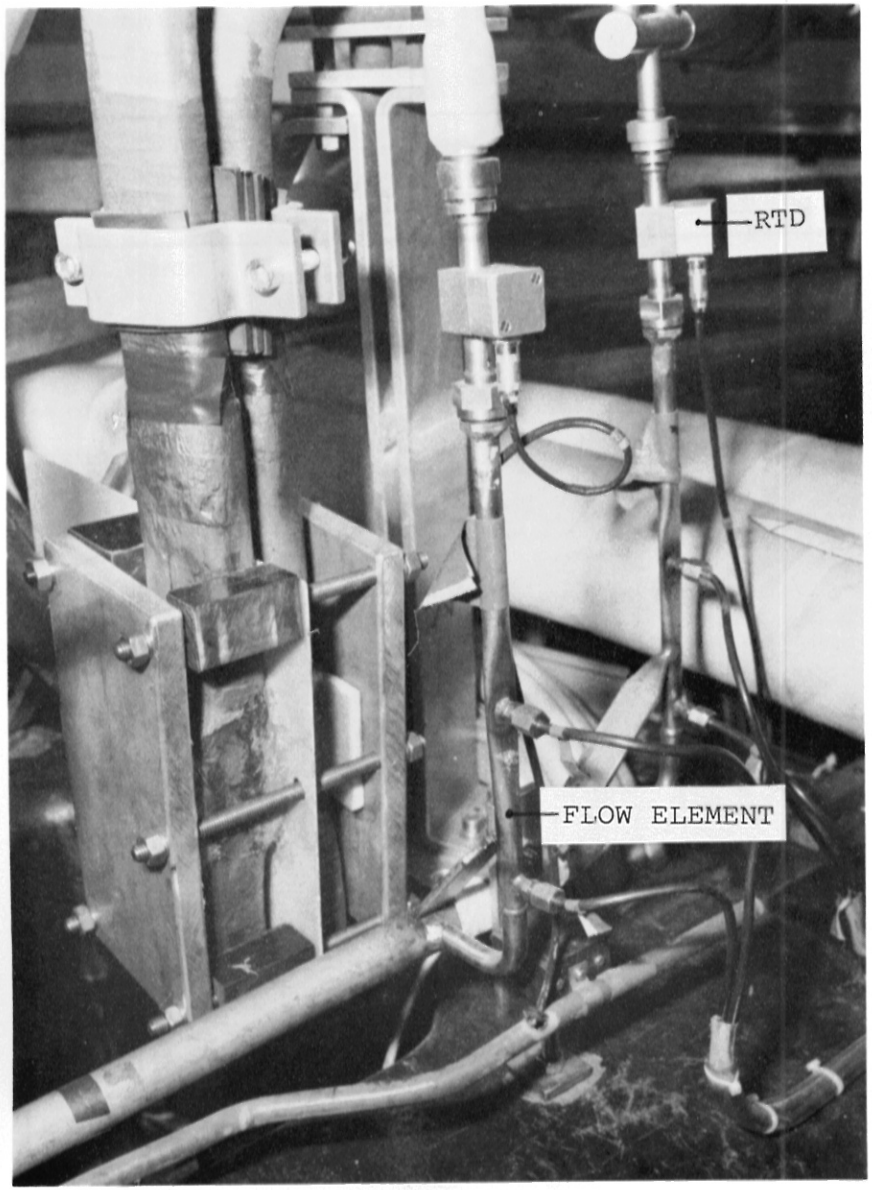

FIG. 8: PHOTOGRAPH OF RTD AND FLOW ELEMENT
(FOR DESIGN SEE FIG.6 AND FIG.10)

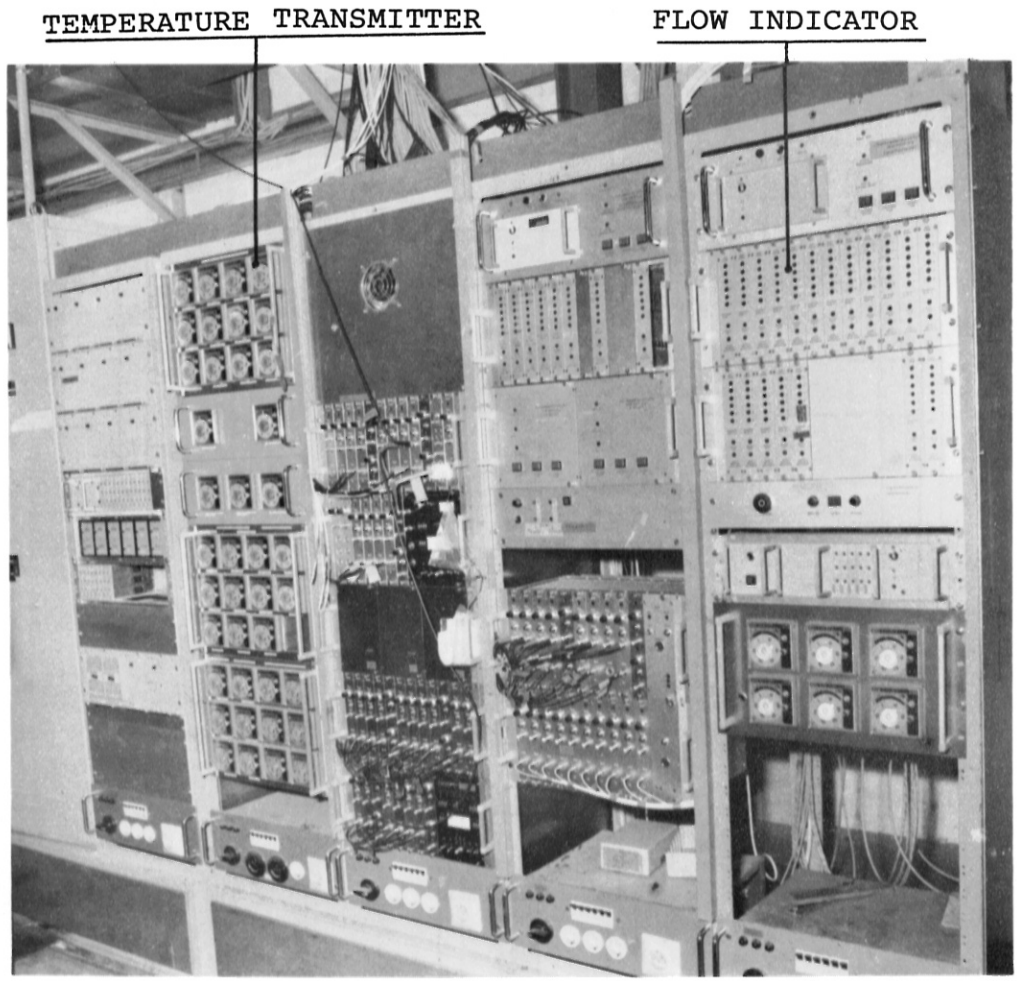

FIG. 9: CONTROL RACKS LOCATED IN THE BASEMENT

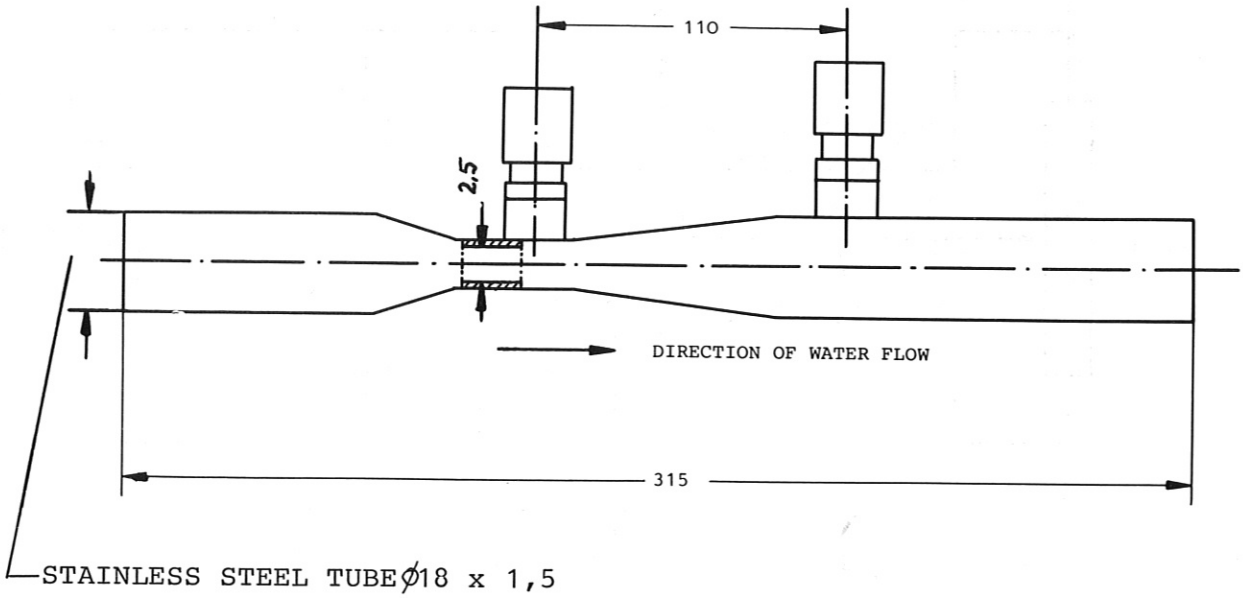

FIG. 10: VENTURI FLOW ELEMENT

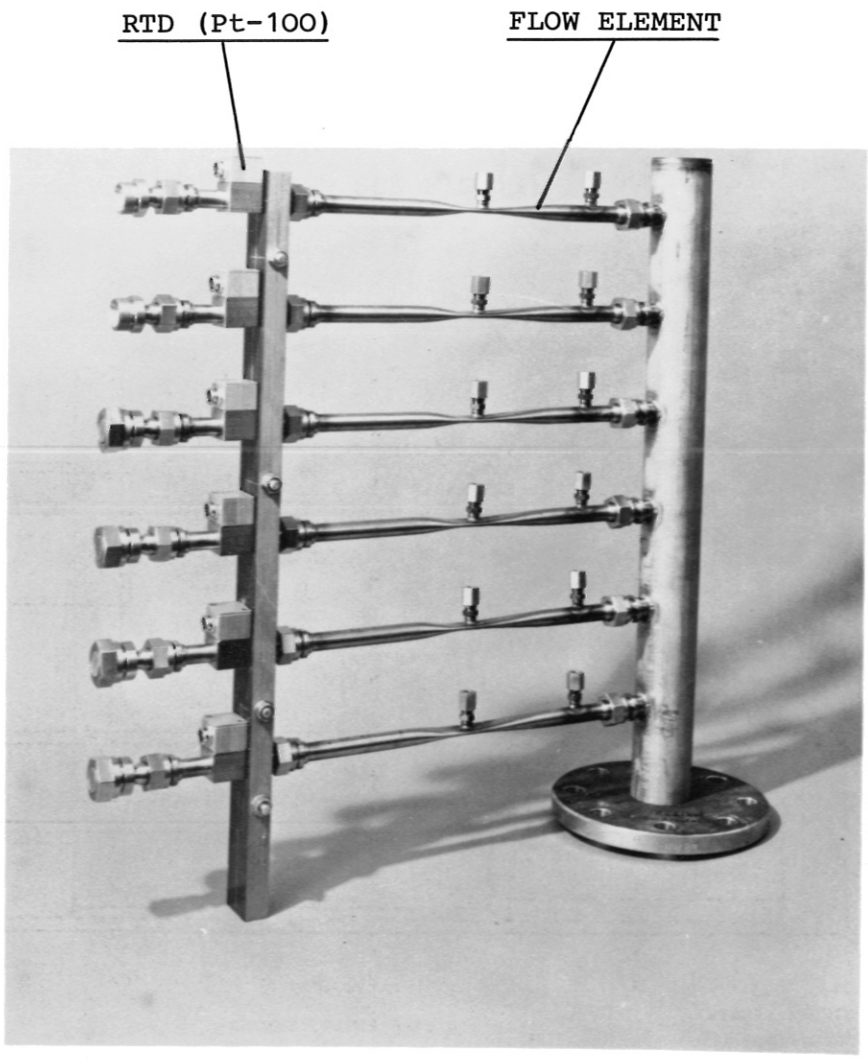

FIG. 11: PHOTOGRAPH OF VENTURI FLOW ELEMENT
(FOR DESIGN SEE FIG.10)

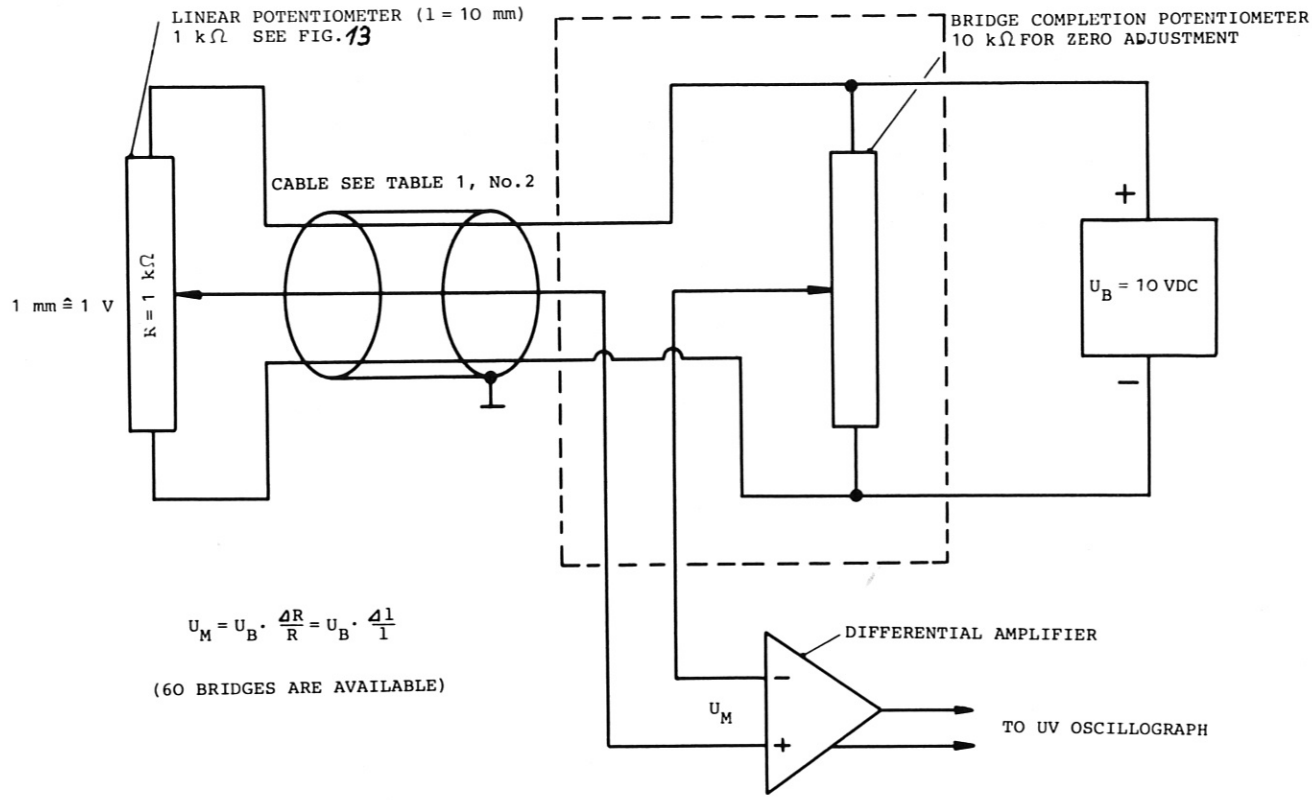

FIG. 12: Bridges for displacement measurement

IPP3 GHT 290-80

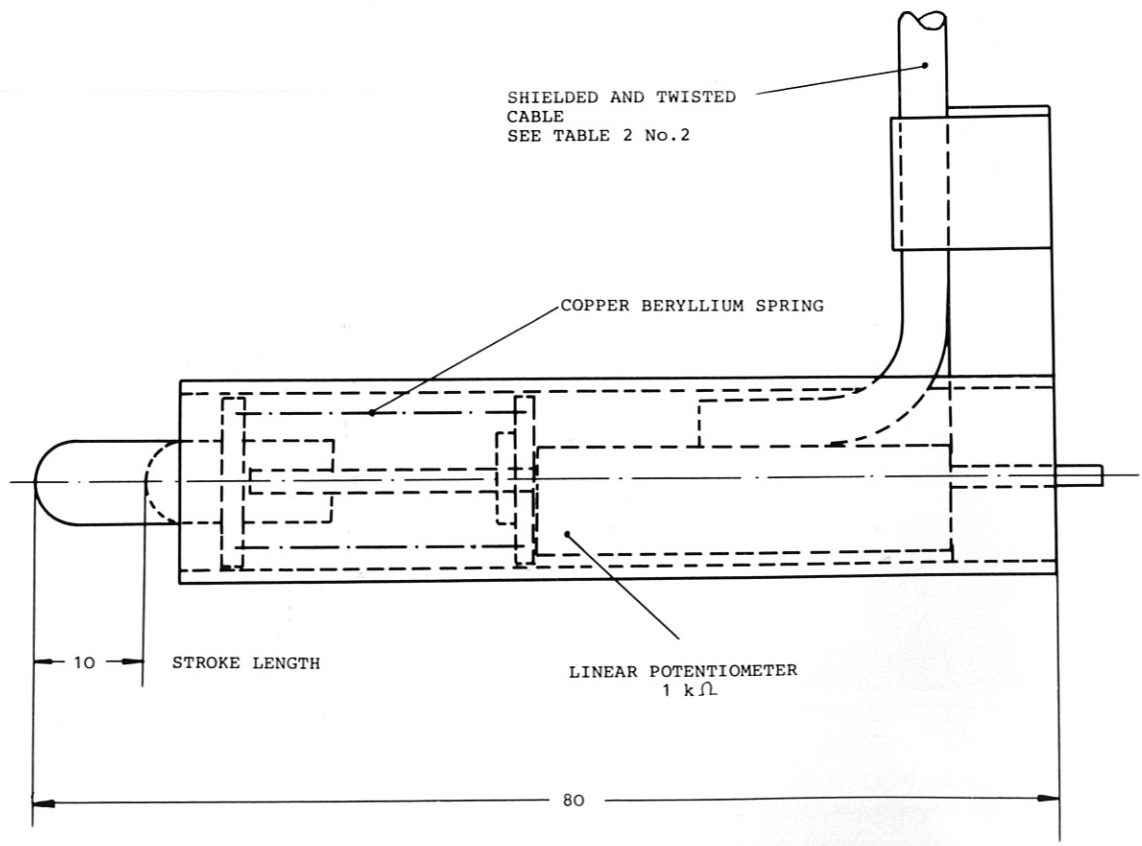

FIG. 13: Linear potentiometer to measure displacements from 50 µm to 10 mm

IPP3 GHT289-80

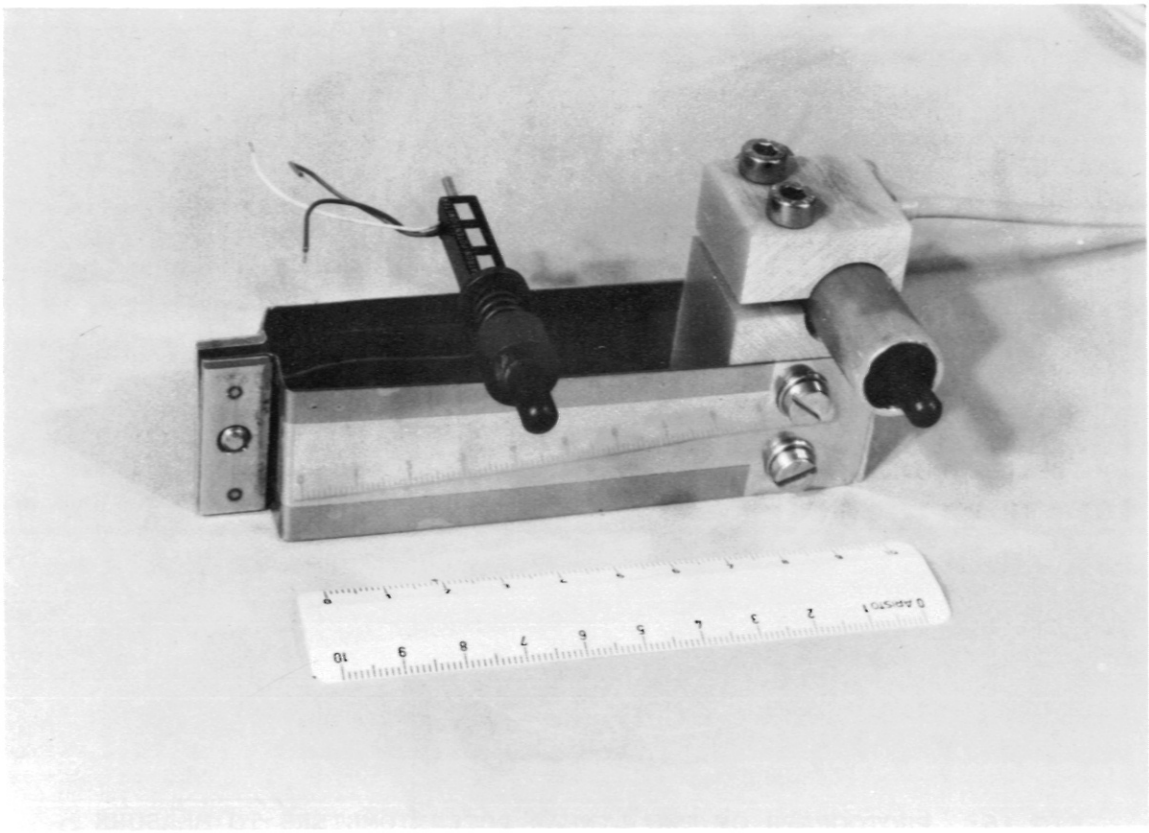

FIG. 14: PHOTOGRAPH OF LINEAR POTENTIOMETER
(FOR DESIGN SEE FIG.13)

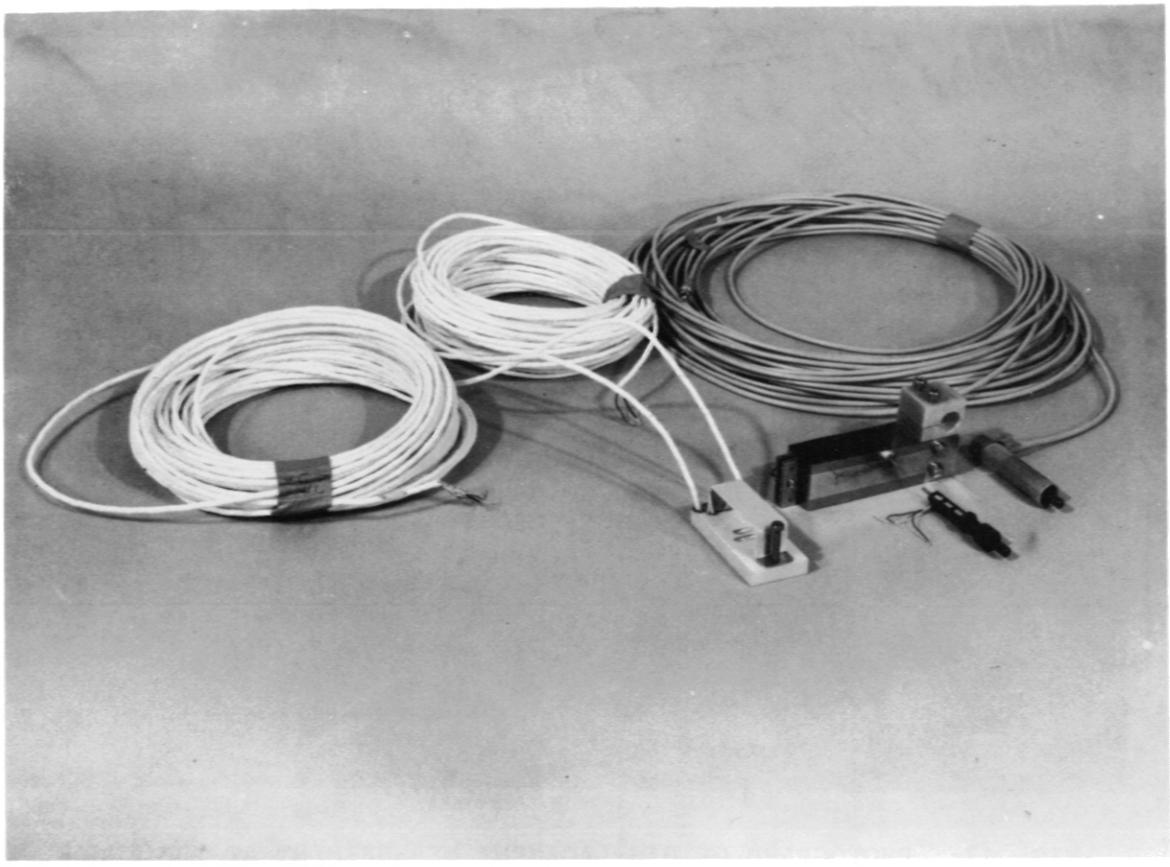

Fig. 15: LINEAR POTENTIOMETER FOR INNER VERTICAL AND DIVERTOR COMPENSATION COILS AND SURFACE RTD FOR RADIAL FIELD COIL
(FOR DESIGN SEE FIG.13)

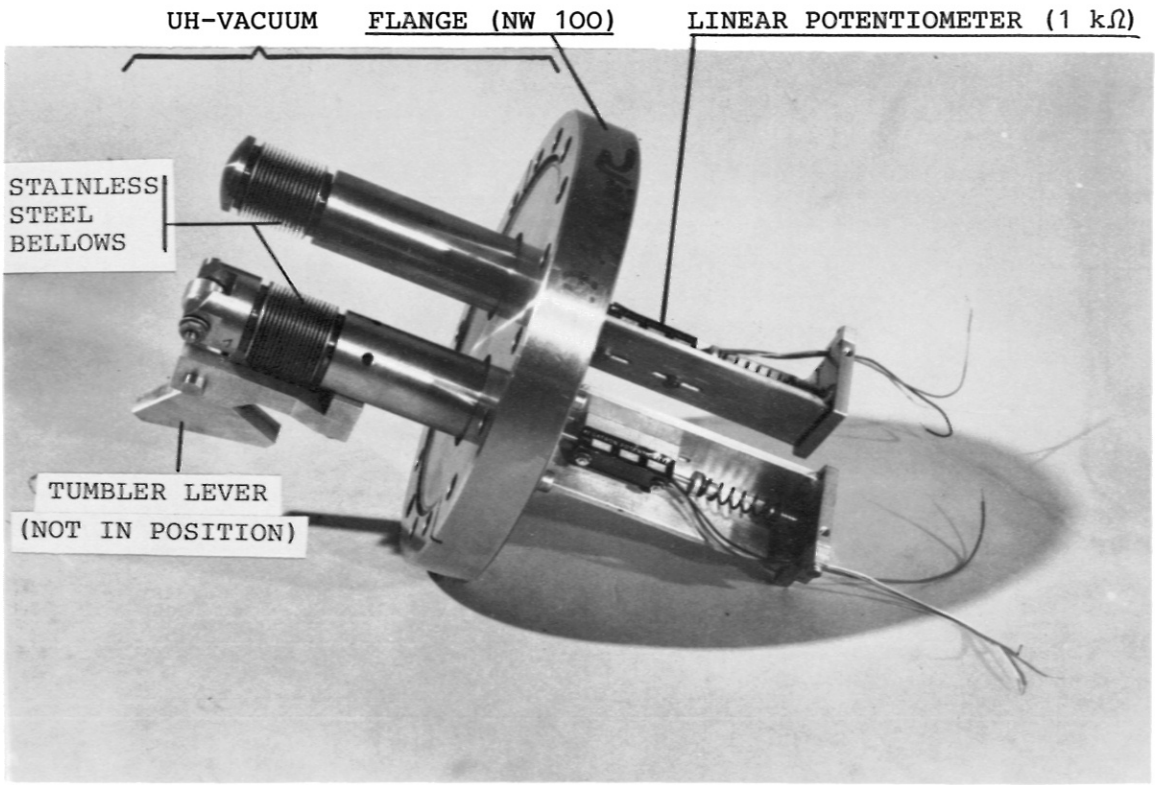

FIG.16: PHOTOGRAPH OF TWO LINEAR POTENTIOMETERS TO MEASURE THE DISPLACEMENT (10 mm) IN THE φ- AND ρ-DIRECTIONS OF THE GETTER PANEL

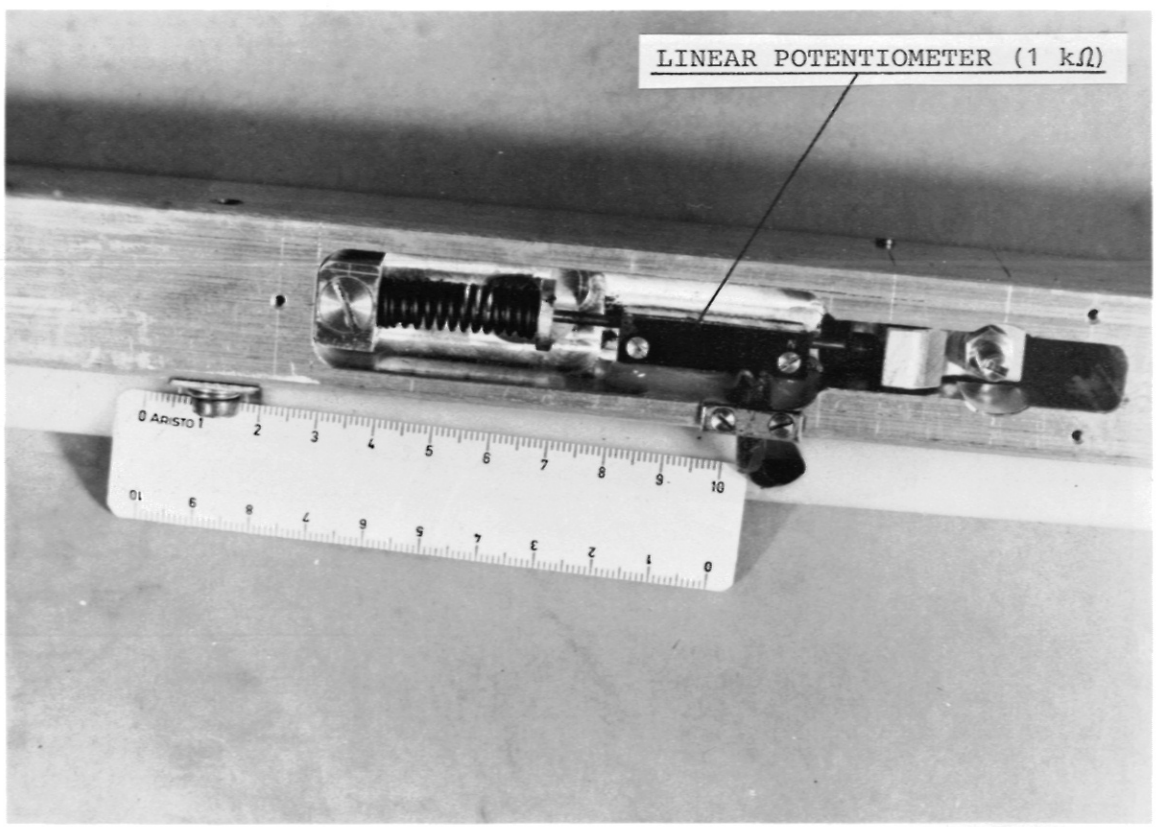

FIG. 17: PHOTOGRAPH OF DISPLACEMENT MEASUREMENT AT THE INNER OHMIC HEATING COILS, VIEW A (FOR DESIGN SEE FIG.18)

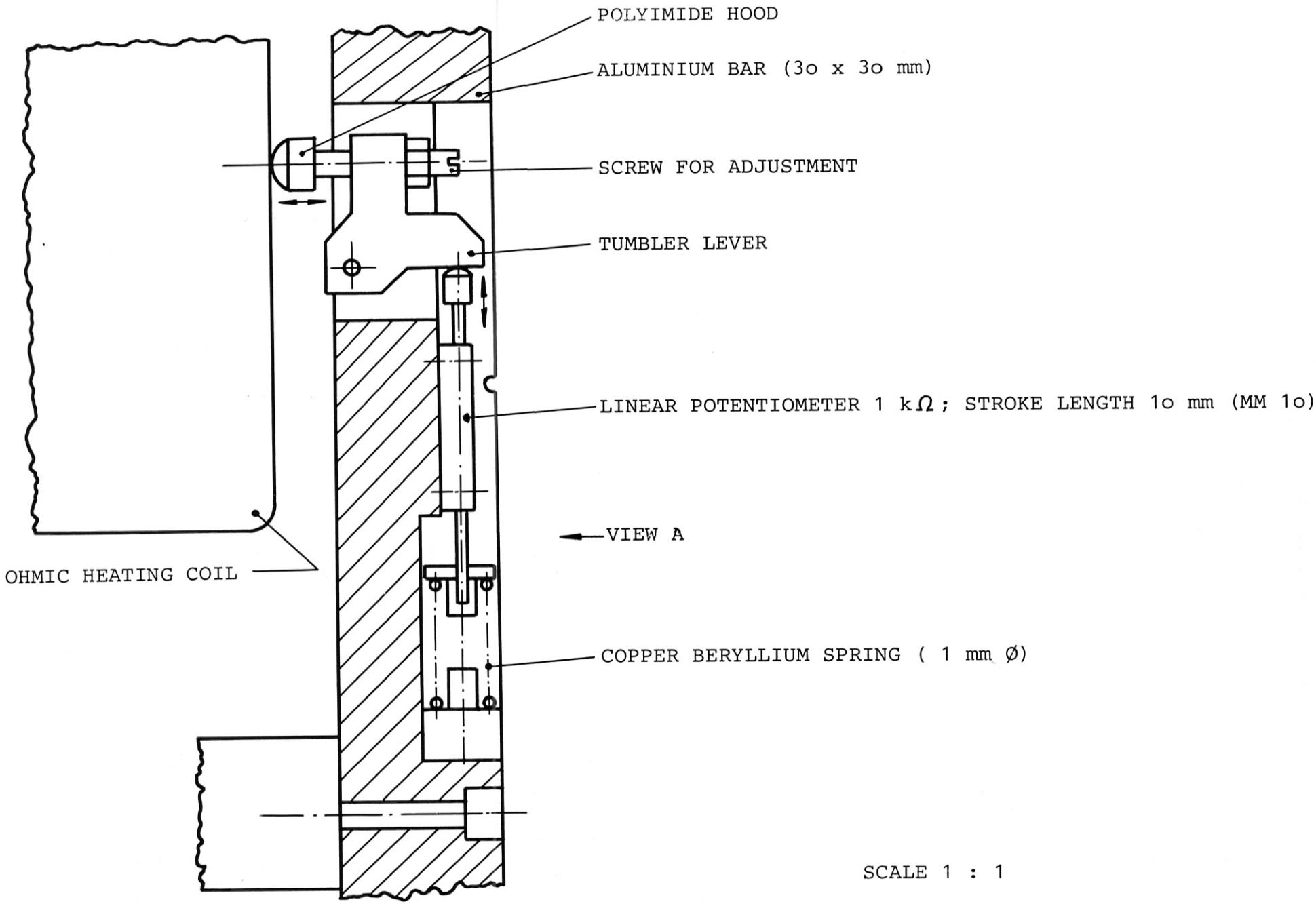

FIG. 18: LINEAR POTENTIOMETER ARRANGEMENT TO MEASURE DISPLACEMENT IN THE INNER OHMIC HEATING COILS

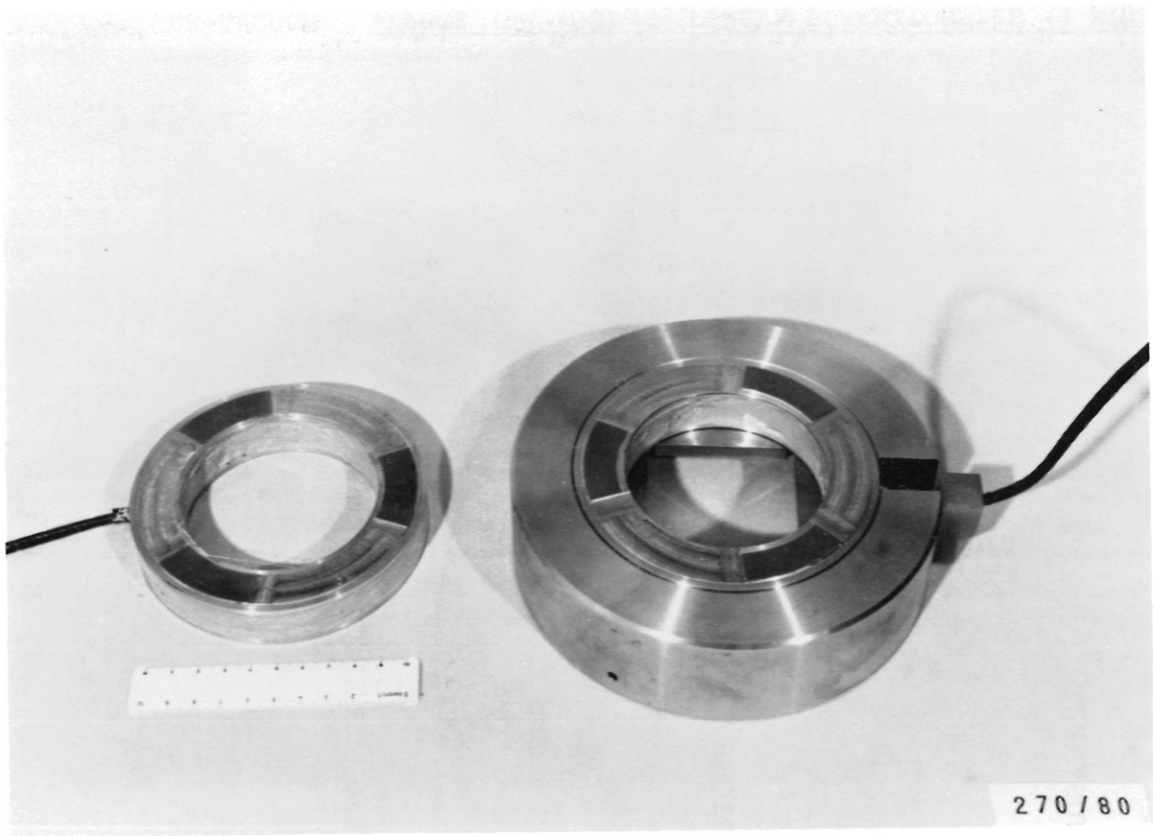

FIG: 19: PRESSURE TRANSDUCERS TO MEASURE THE WEIGHT DISTRIBUTION OF THE VACUUM VESSEL AT 8 POINTS (HIGH 20 mm)

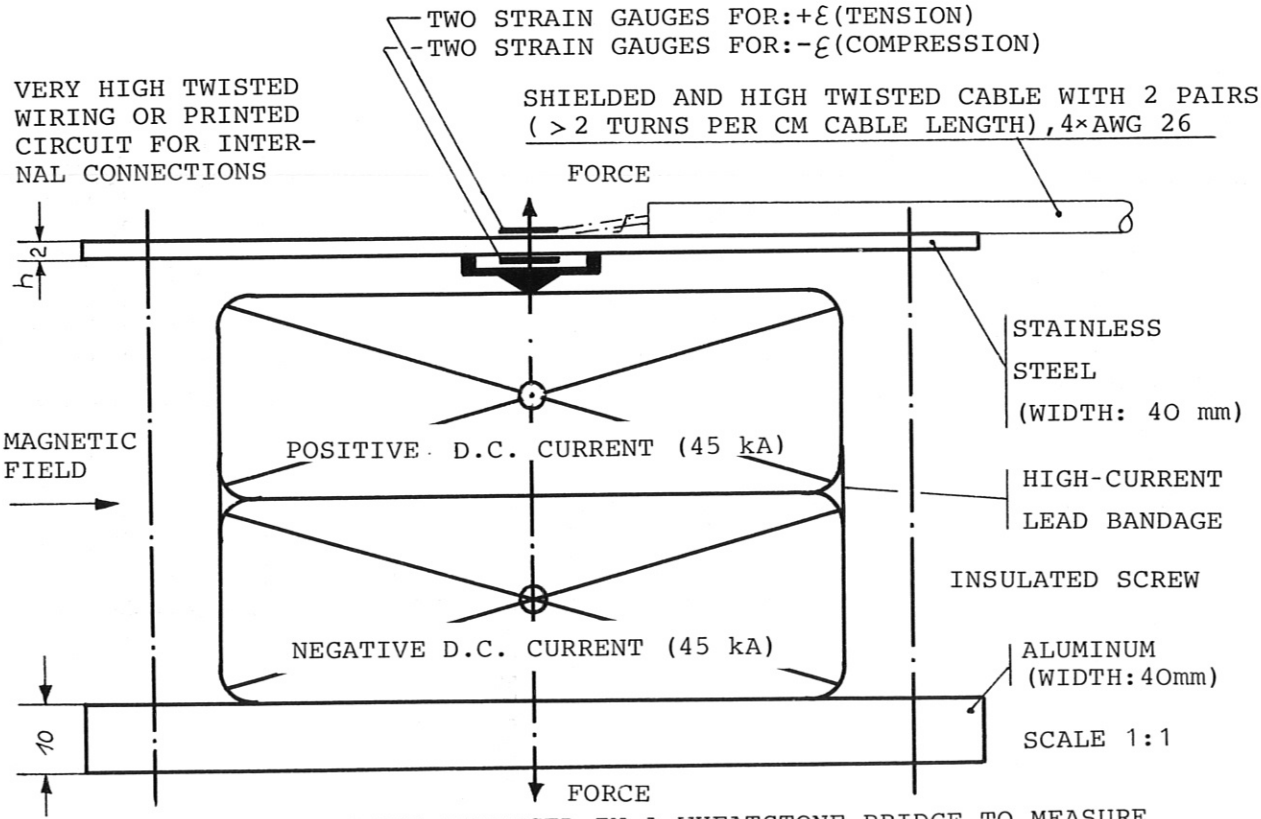

FIG. 19a: STRAIN GAUGE ARRANGED IN A WHEATSTONE BRIDGE TO MEASURE DISPLACEMENT (STRAIN) ON HIGH-CURRENT LEADS

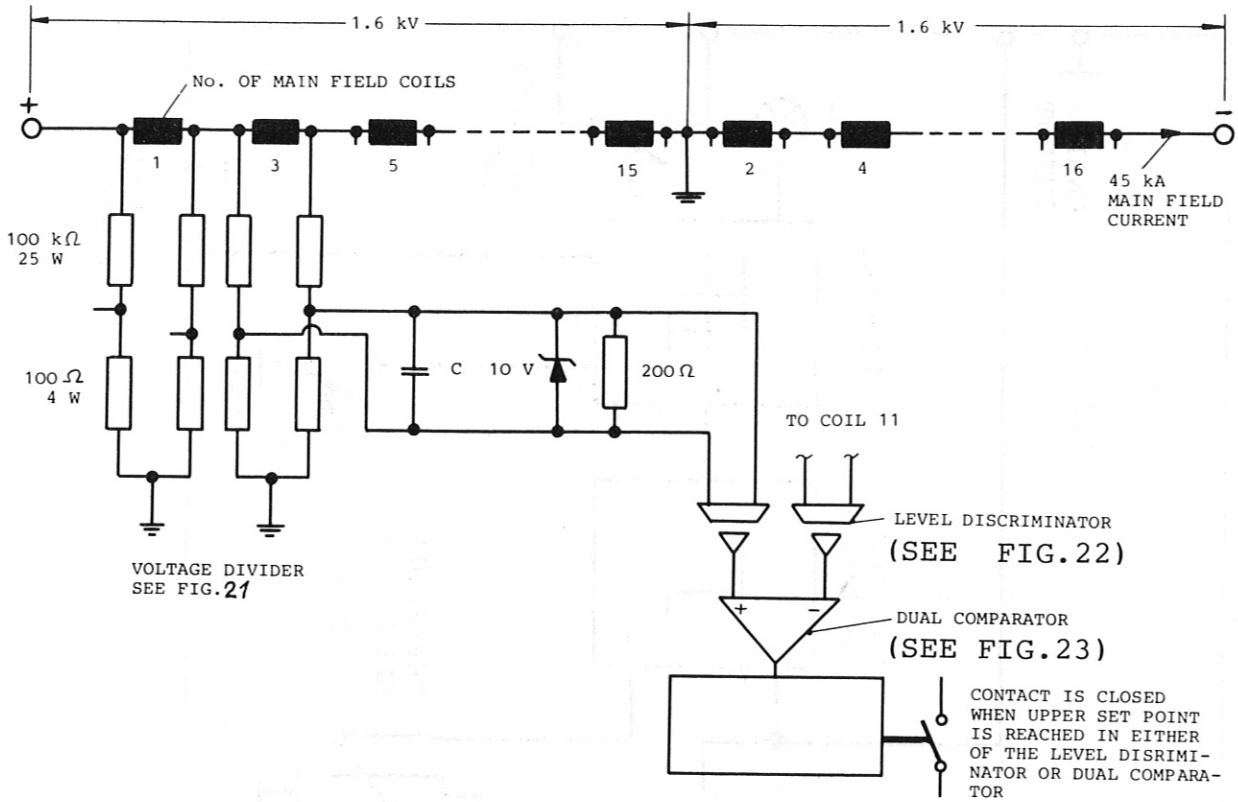

FIG. 20: VOLTAGE SYMMETRY MEASUREMENT OF THE 16 MAIN FIELD COILS

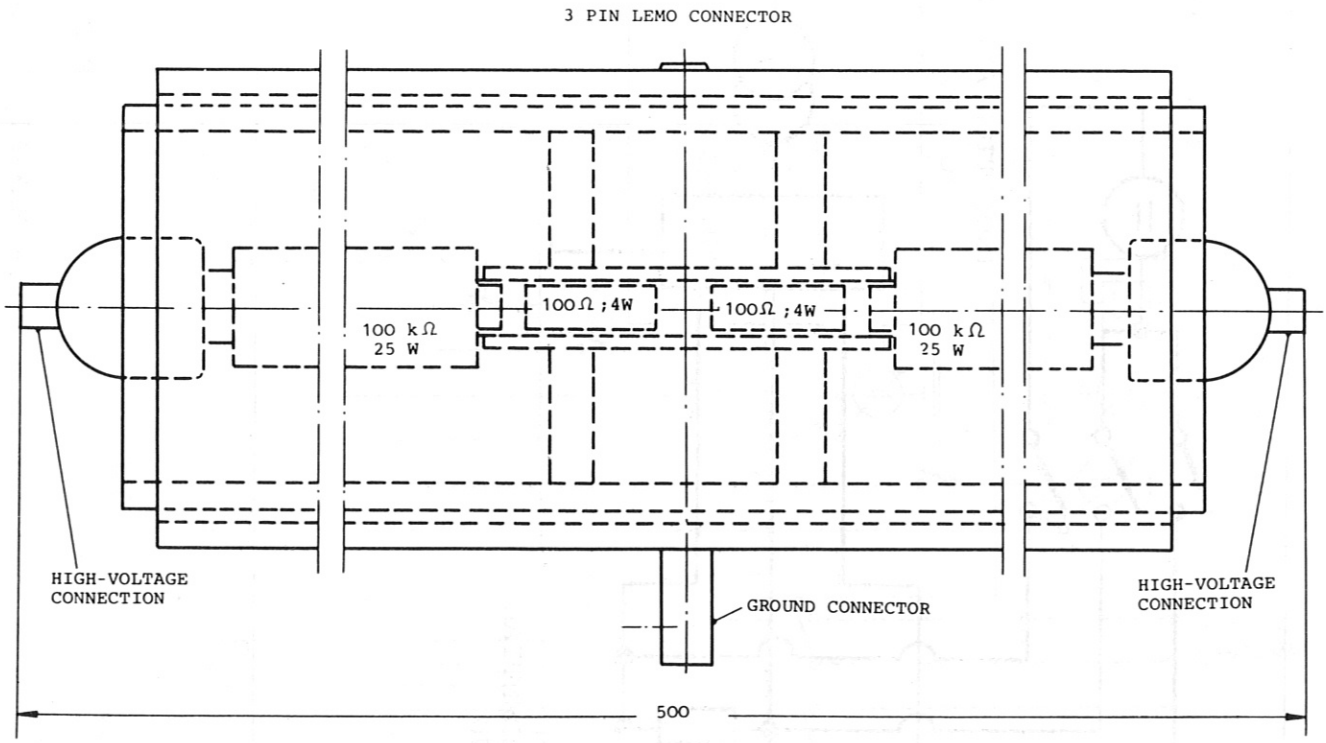

FIG. 21: DIFFERENTIAL VOLTAGE DIVIDER; 0.1% TOLERANCE

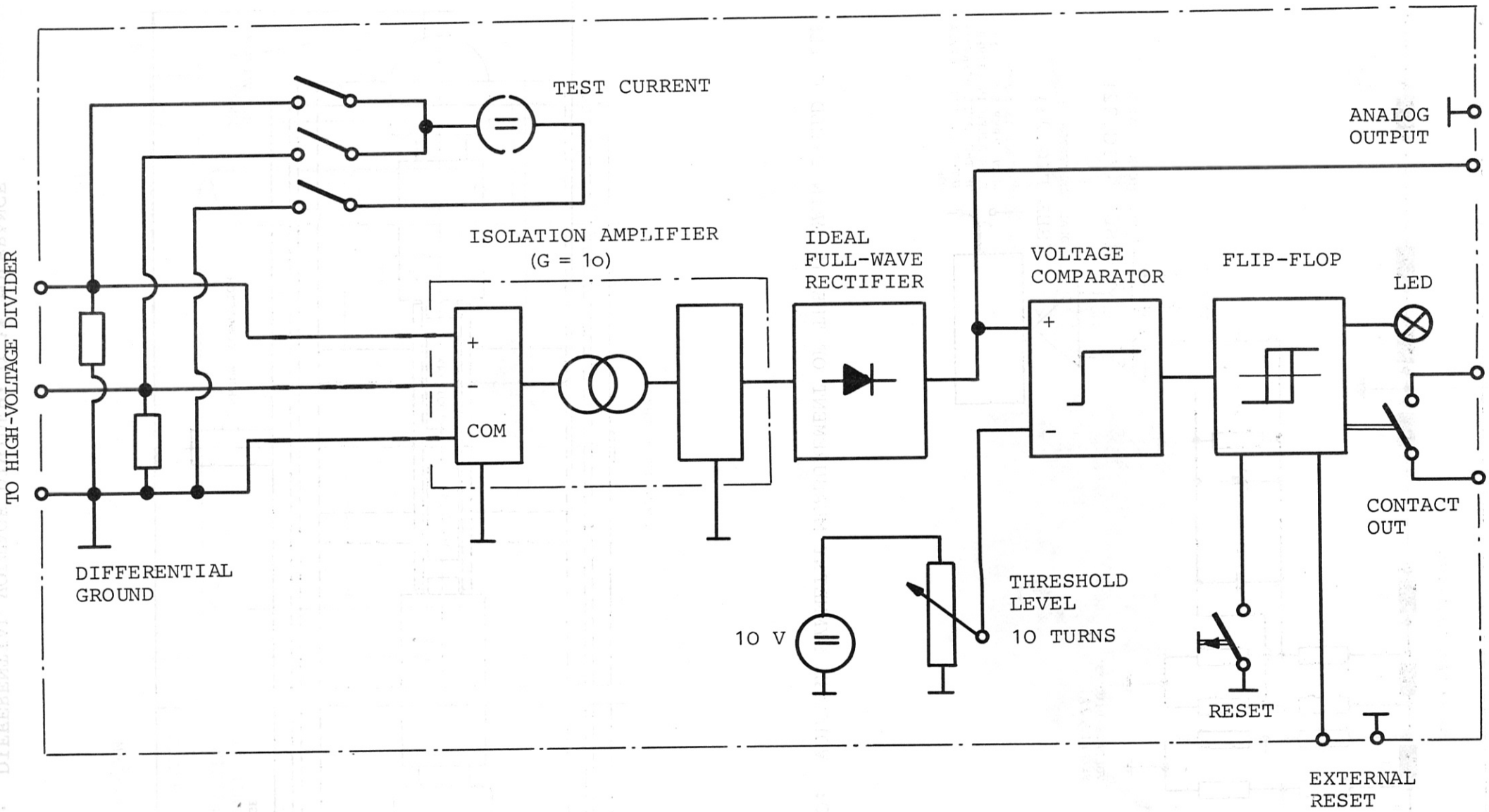

FIG.22:

LEVEL DISCRIMINATOR

FOR MAXIMUM MEASUREMENT (SYMMETRICAL VOLTAGE)

IPP3 GHT 304-80'

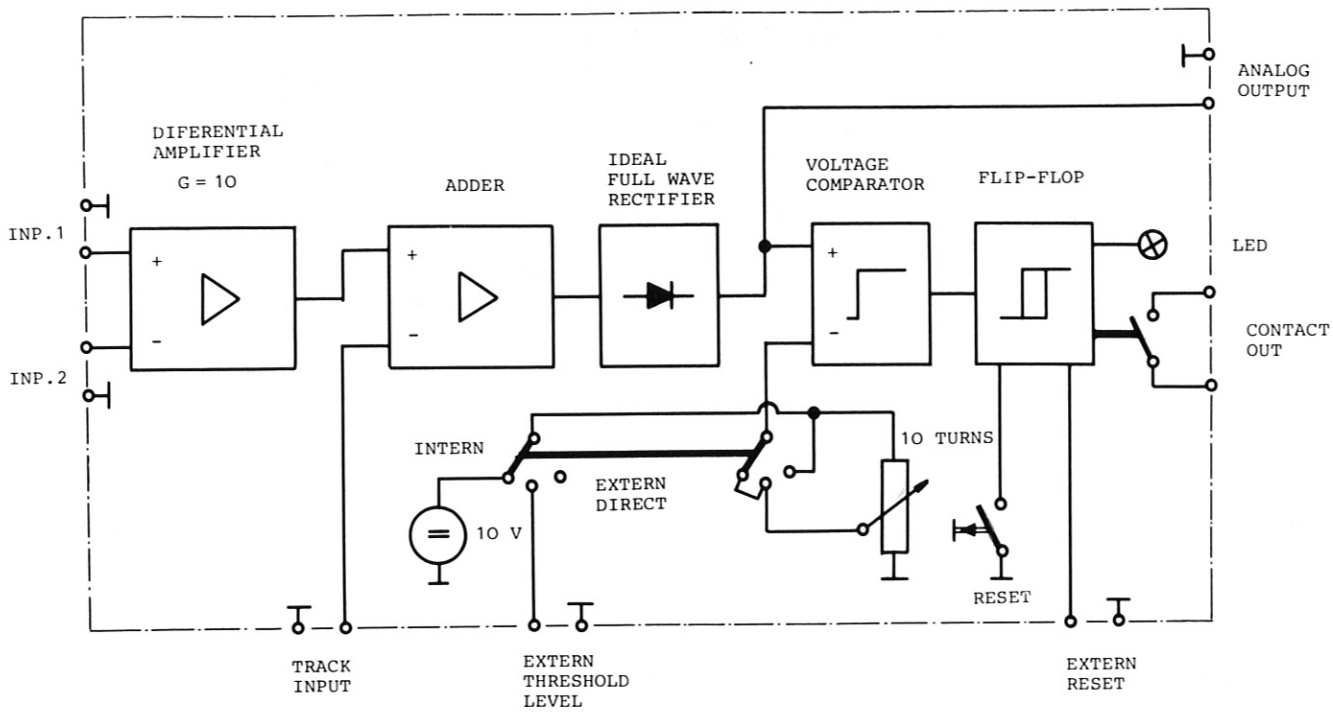

FIG. 23: DUAL COMPARATOR FOR SYMMETRICAL MEASUREMENT (VOLTAGE)

FIG. 24: SELF TEST ASSEMBLY (SYMMETRICAL VOLTAGE)

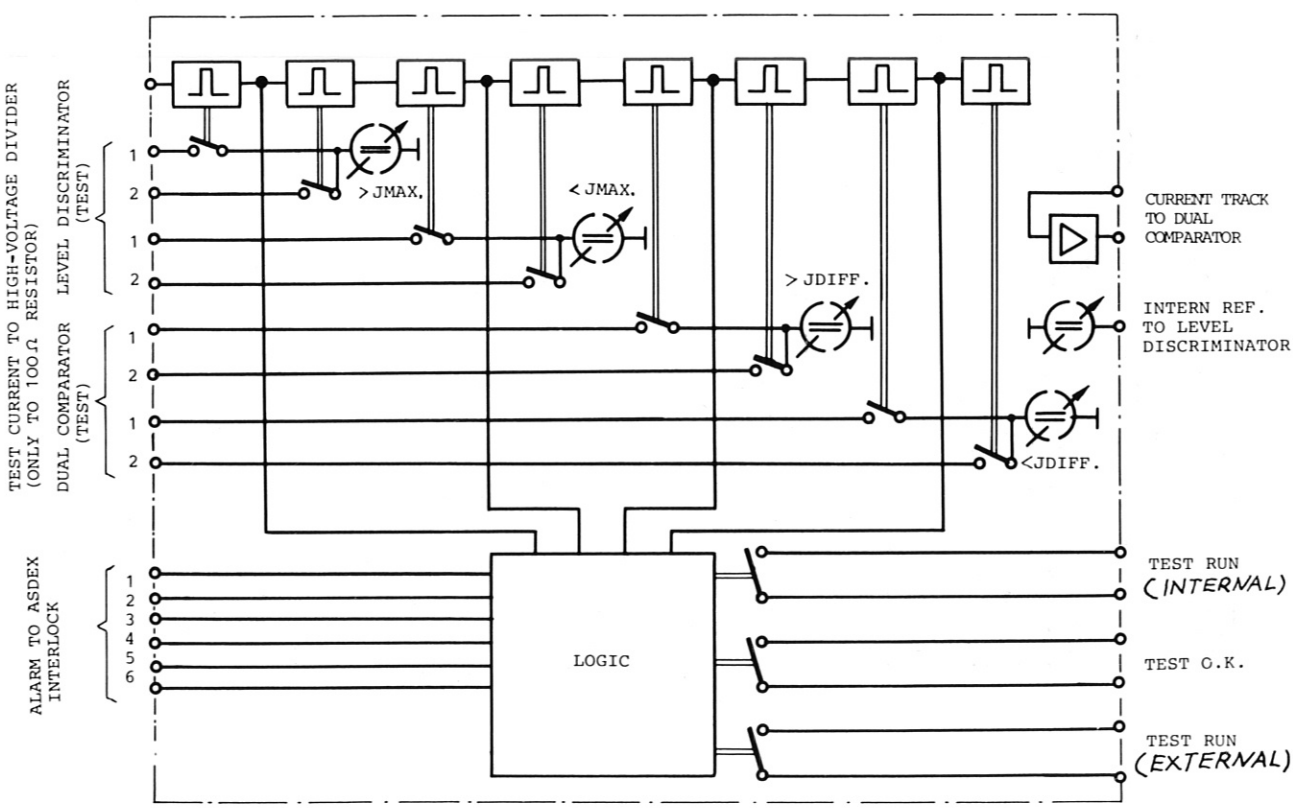

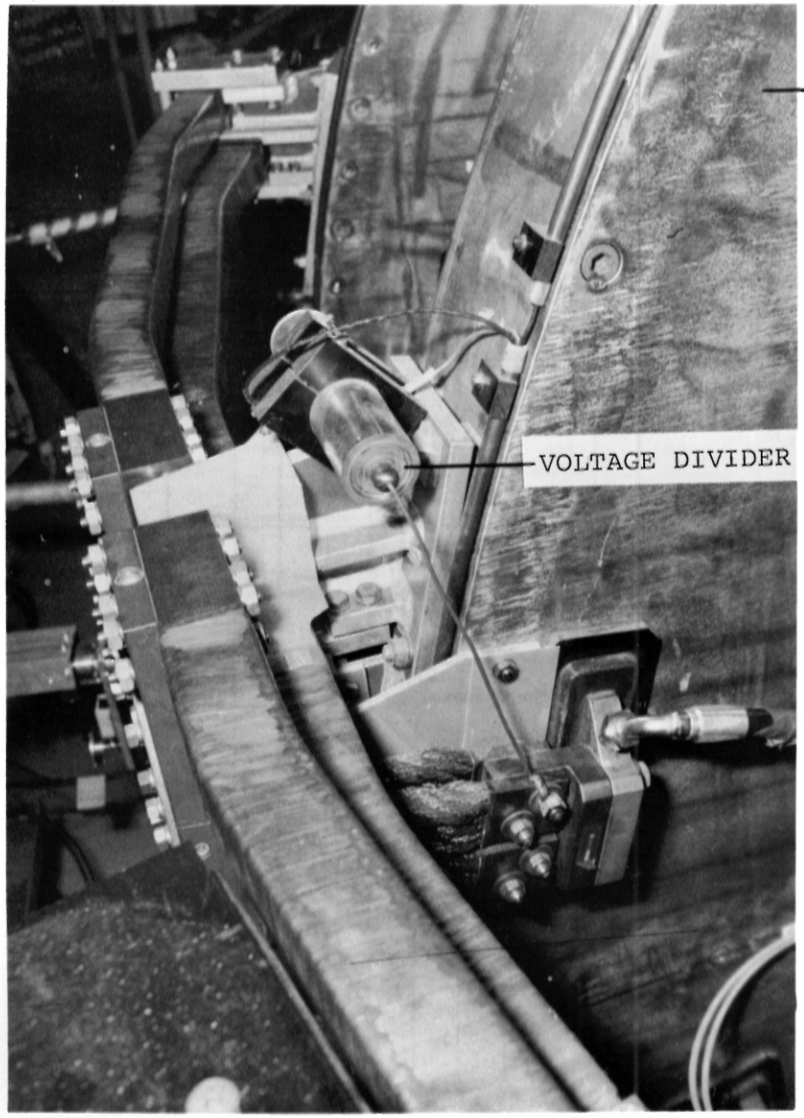

FIG 25:
PHOTOGRAPH OF DIFFERENTIAL VOLTAGE DIVIDER MOUNTED AT THE OUTSIDE OF THE MAIN FIELD COIL
(FOR DESIGN SEE FIG. 21)

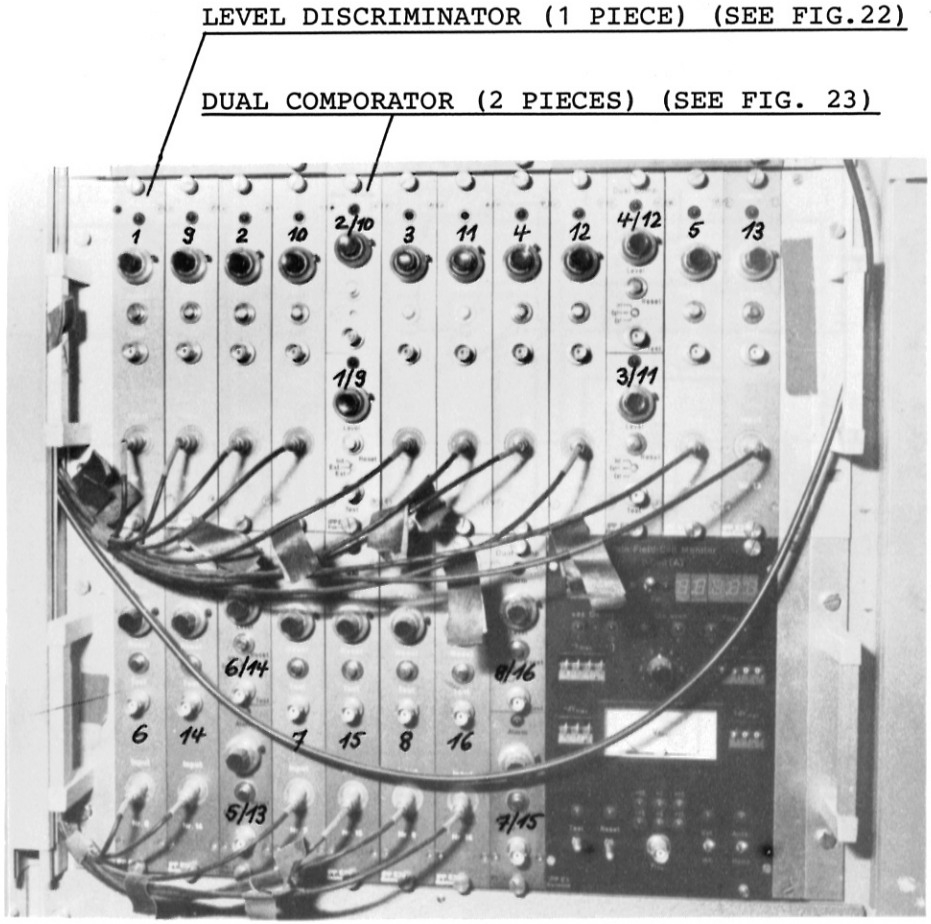

FIG.26: SELF TEST UNIT; DISCRIMINATORS AND COMPARATORS MOUNTED IN A NIM CREATE (SYMMETRICAL VOLTAGE)

FIG.27: TEST VOLTAGES FOR SELF TEST ASSEMBLY

(SYMMETRICAL VOLTAGE) SEE FIG.24

TEST POSITION AUTOMATIC OR MANUAL	TEST VOLTAGE	TEST CURRENT TO LEVEL DISCRIMINATOR CONNECTED TO VOLTAGE DIVIDER ON MAIN FIELD COIL No.				REACTION ON			
						LEVEL DISCRIMINATOR		DUAL COMPARATOR	
		1 - 8		9 - 16		LED		LED	
		Pos	Neg.	Pos.	Neg.	on	out	on	out
1a	+ΔVmax	x					x	x	
1b	+ΔVmax		x				x	x	
2a	+ΔVmax			x			x	x	
2b	+ΔVmax				x		x	x	
3a	-ΔVmax	x					x		x
3b	-ΔVmax		x				x		x
4a	-ΔVmax			x			x		x
4b	-ΔVmax				x		x		x
5a	- Vmax	x		x			x		x
5b	- Vmax		x		x		x		x
6a	+ Vmax	x		x		x			x
6b	+ Vmax		x		x	x			x

1.) +ΔVmax (max.99.9V) differential test voltage at the main field coils. This test voltage should exceed the voltage setting on the dual comparator potentiometer.

2.) -ΔVmax (min.99.9V) differential test voltage at the main field coils. This test voltage should not exceed the voltage setting on the dual comparator potentiometer.

3.) + Vmax (max.999.9V) positive test voltage at the main field coils. This test voltage should exceed the voltage setting on the level discriminator potentiometer.

4.) - Vmax (min.999.9V) negative test voltage at the main field coils. This test voltage should not exceed the voltage setting on the level discriminator potentiometer.

5.) Set point (SL) for level discriminator

$$SL = k \times 100 \qquad k \triangleq \text{potentiometer setting}$$

6.) Set point (SC) for dual comparator

$$SC = k \times 10\ [V] \times \frac{J_{\varphi}\ [A]}{45000\ [A]}$$

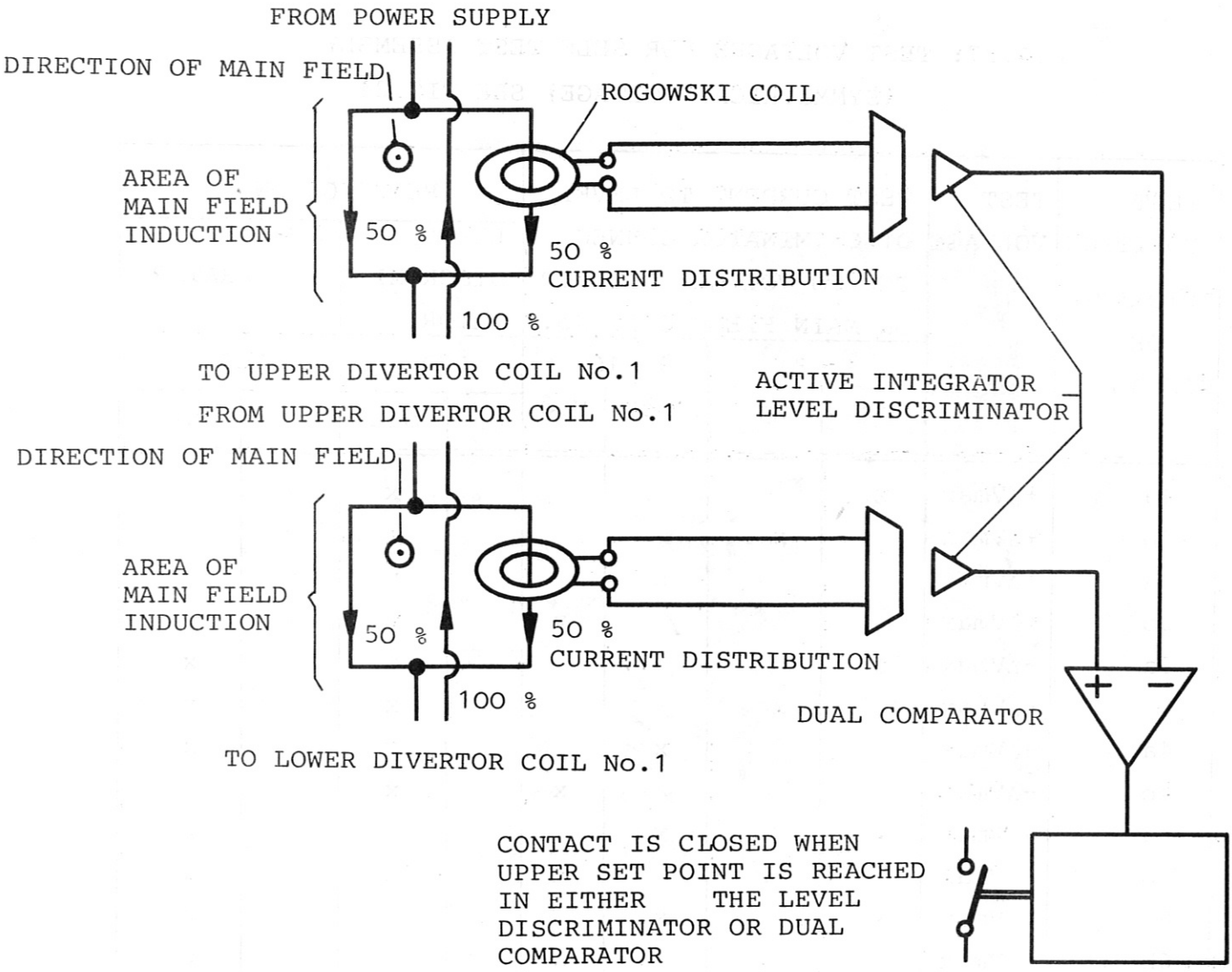

FIG.28: CURRENT SYMMETRY OF UPPER AND LOWER DIVERTOR COILS

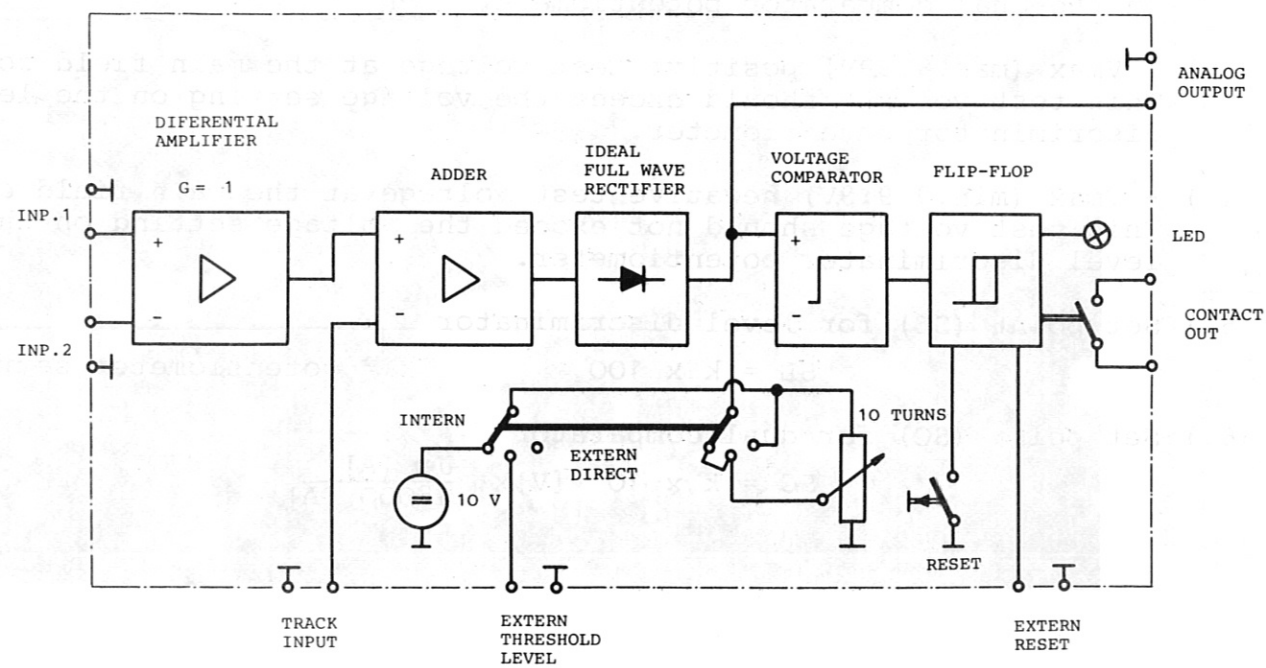

FIG. 29: DUAL COMPARATOR FOR SYMMETRICAL MEASUREMENT (CURRENT)
(FOR CIRCUIT DESIGN SEE FIG. 28)

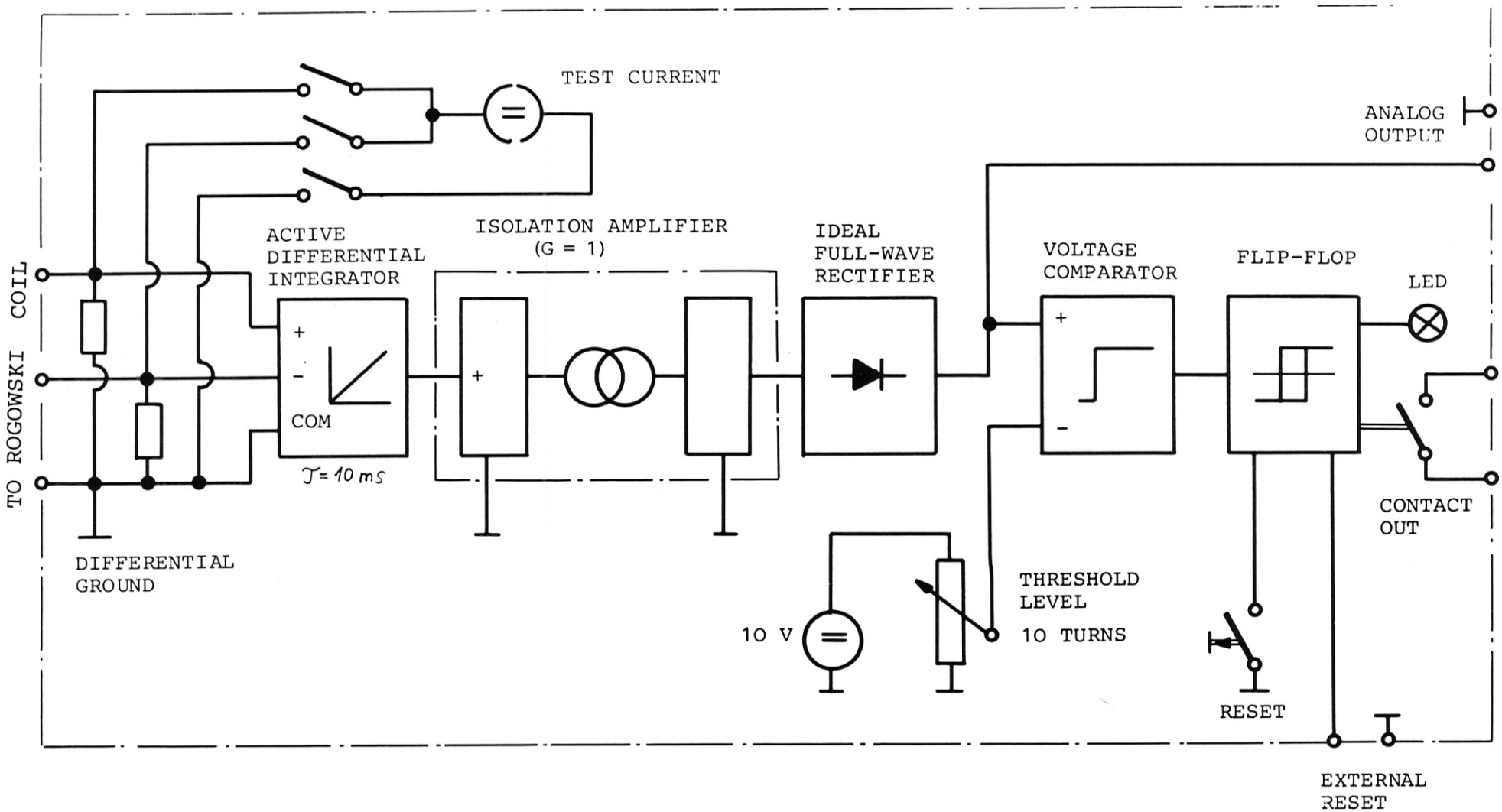

IPP3 GHT 305-80

FIG. 30: INTEGRATOR, LEVEL DISCRIMINATOR FOR MAXIMUM MEASUREMENT (SYMMETRICAL CURRENT)

FOR CIRCUIT DESIGN SEE FIG. 28

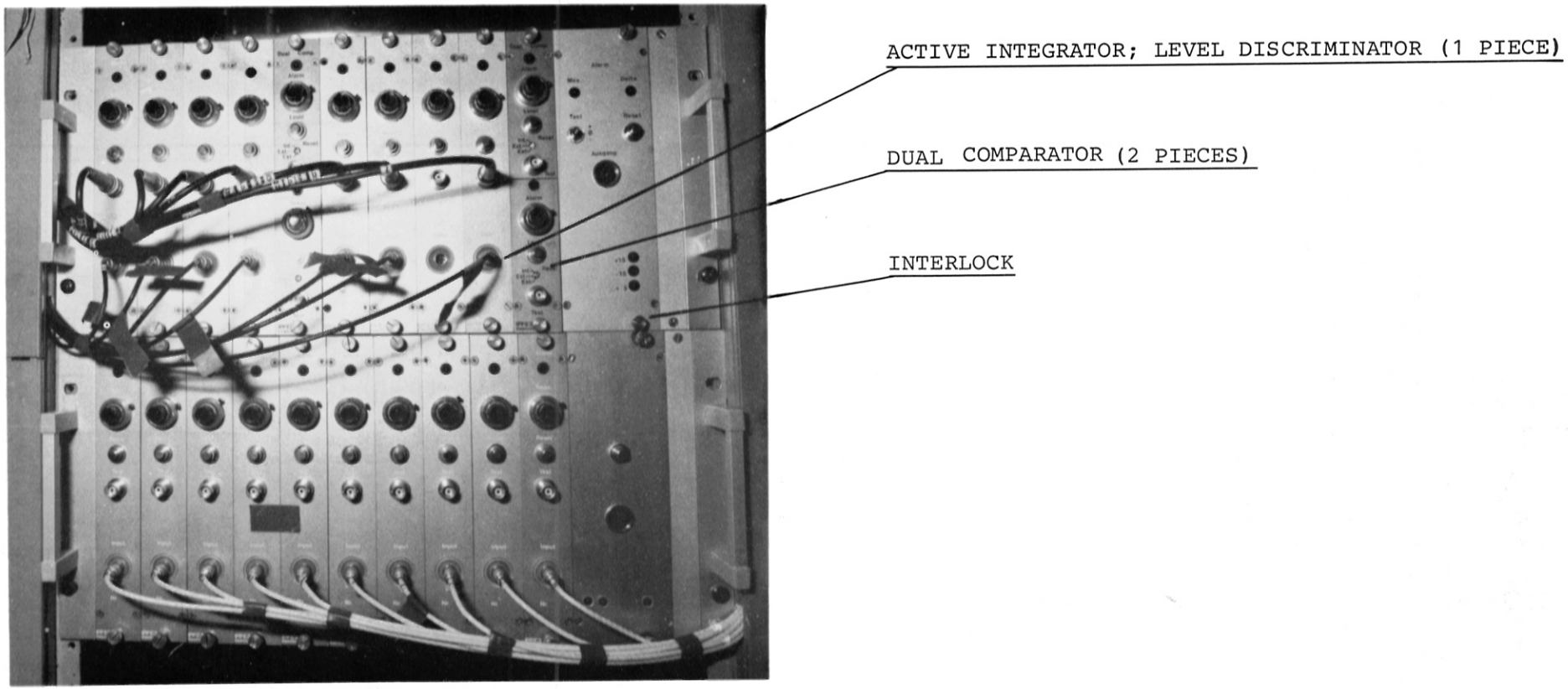

FIG. 31: PHOTOGRAPH OF TEST UNIT AND CONTROL UNITS MOUNTED IN A NIM CRATE (SYMMETRICAL CURRENT)

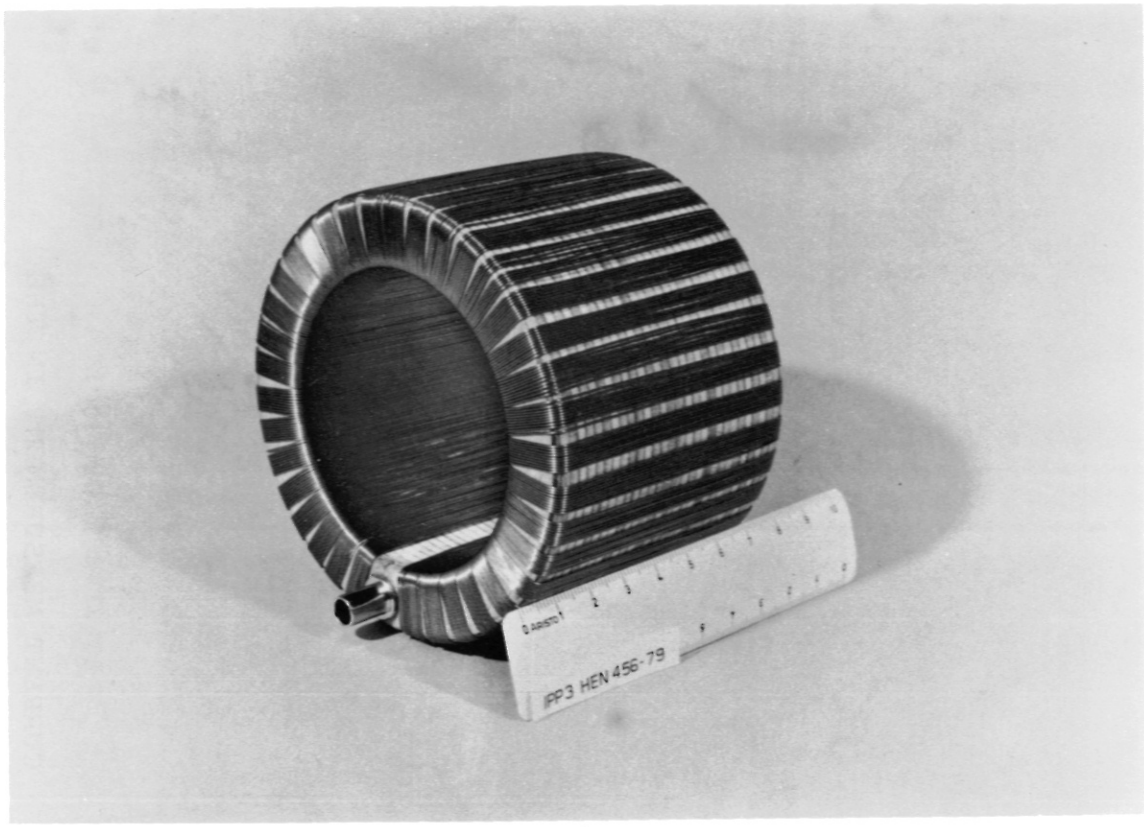

FIG. 32: ROGOWSKI COIL FOR CURRENT MEASUREMENT

FIG.33: ROGOWSKI COIL FOR DIVERTOR COIL MOUNTED ON THE BUSBARS FOR SYMMETRICAL CURRENT MEASUREMENT (FOR CIRCUIT DESIGN SEE FIG.28)

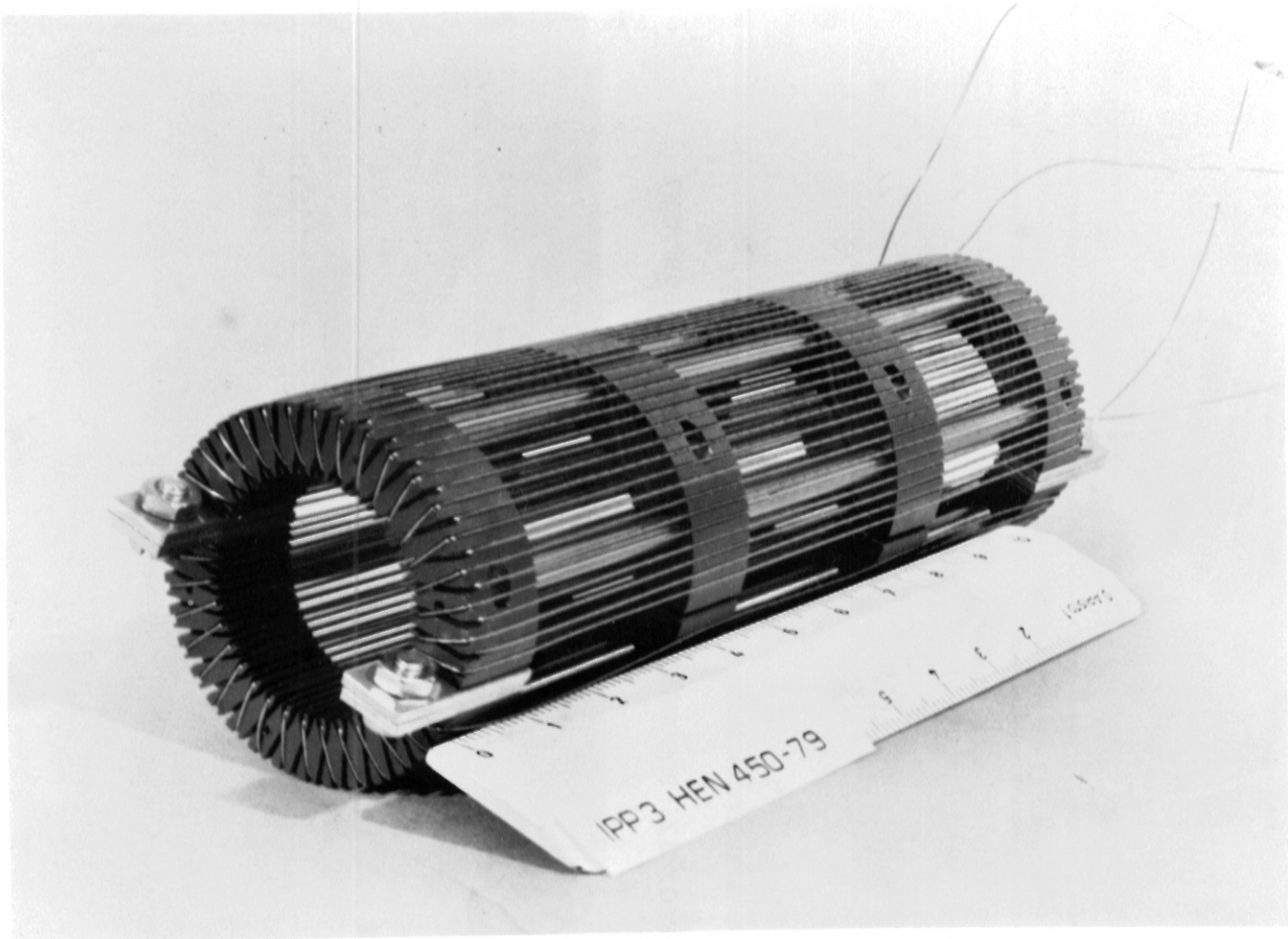

FIG. 34: ROGOWSKI COIL FOR ELECTRIC CURRENT MEASUREMENT IN THE N_2 PIPE MOUNTED IN THE DIVERTOR CHAMBER

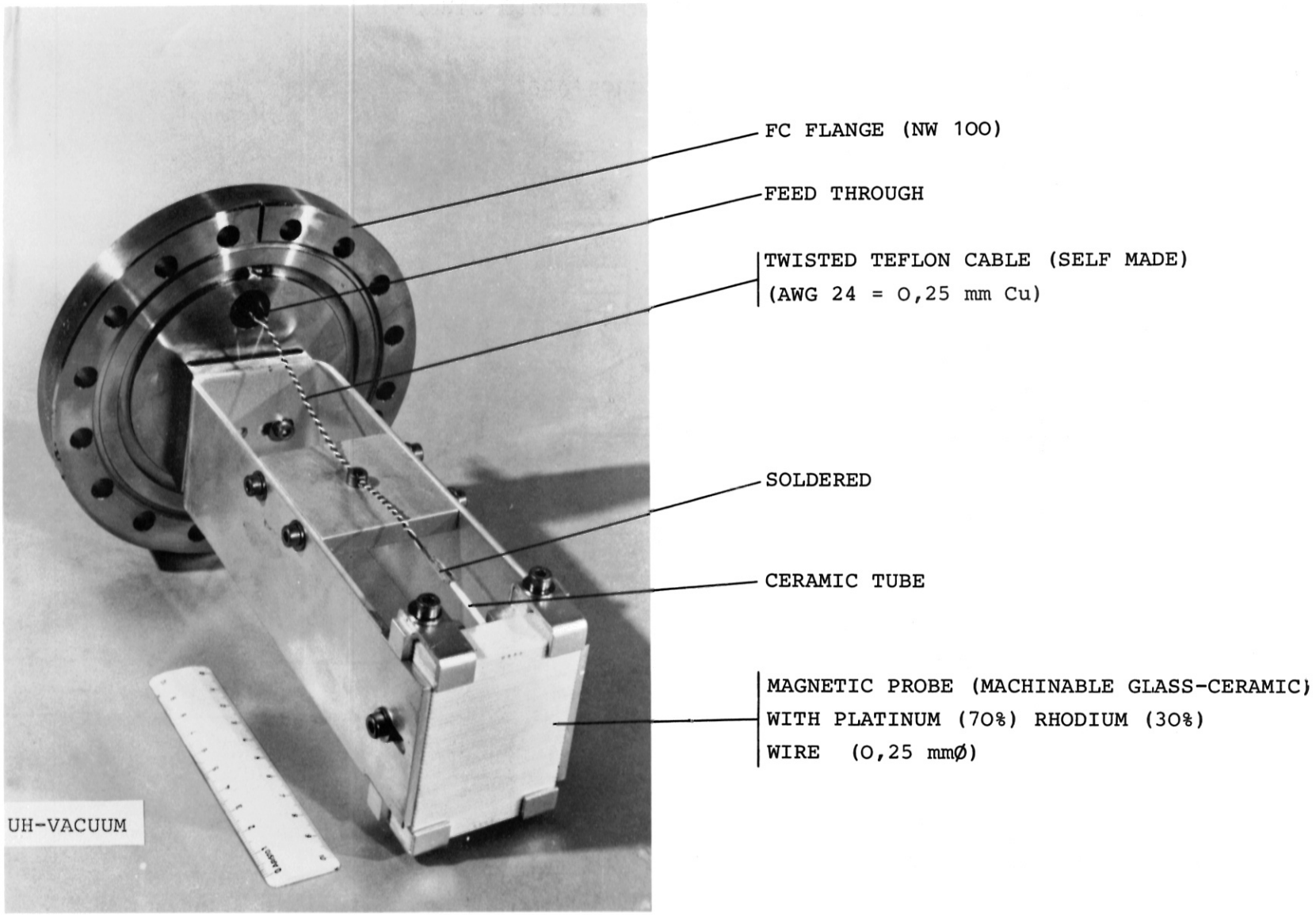

FIG. 35: MAGNETIC PROBE TO MEASURE $\frac{dB}{dt}$ INSIDE THE DIVERTOR CHAMBER

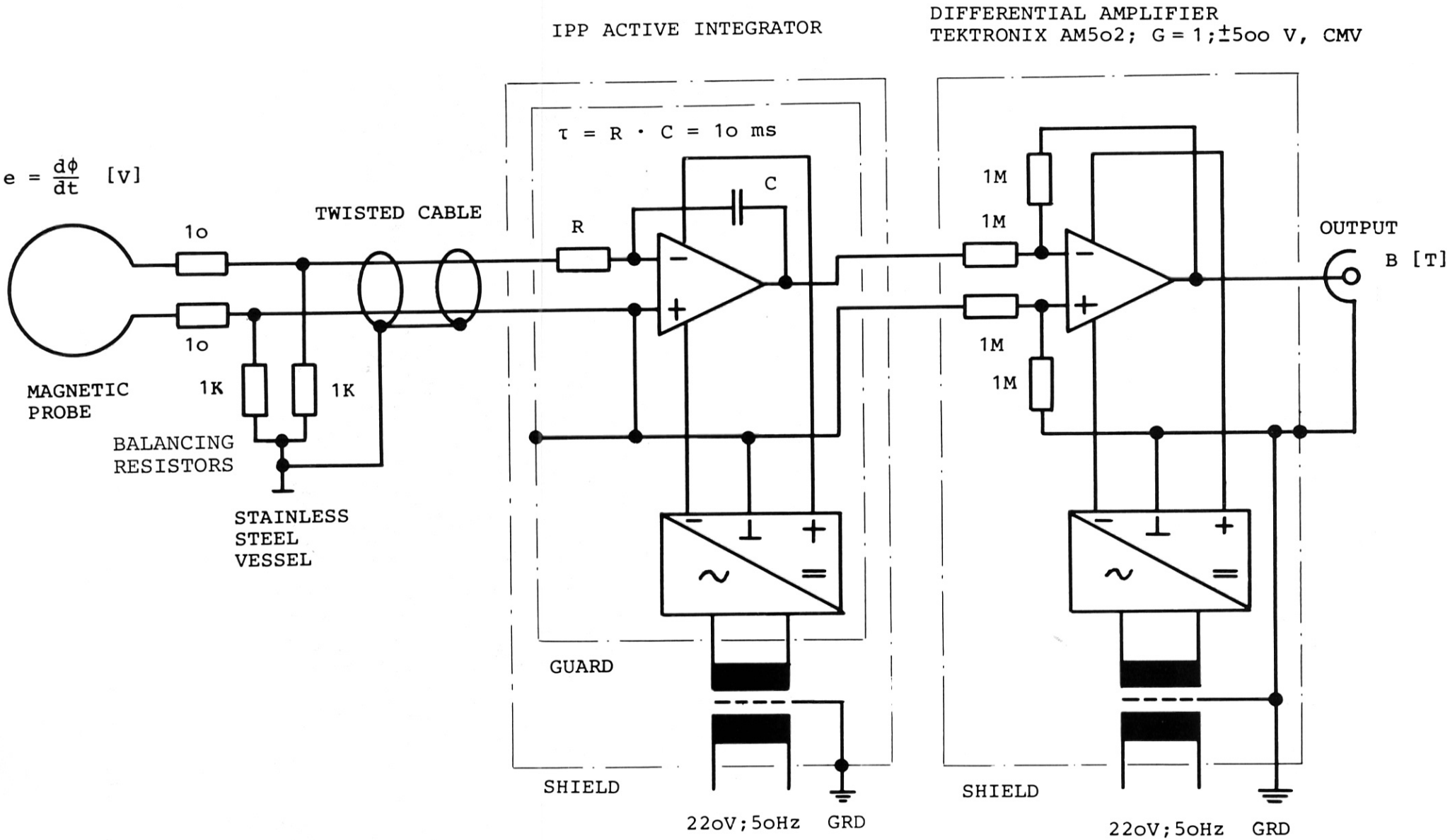

FIG. 36: ELECTRIC CIRCUIT OF MAGNETIC PROBE

IPP 3 GHT 550-80

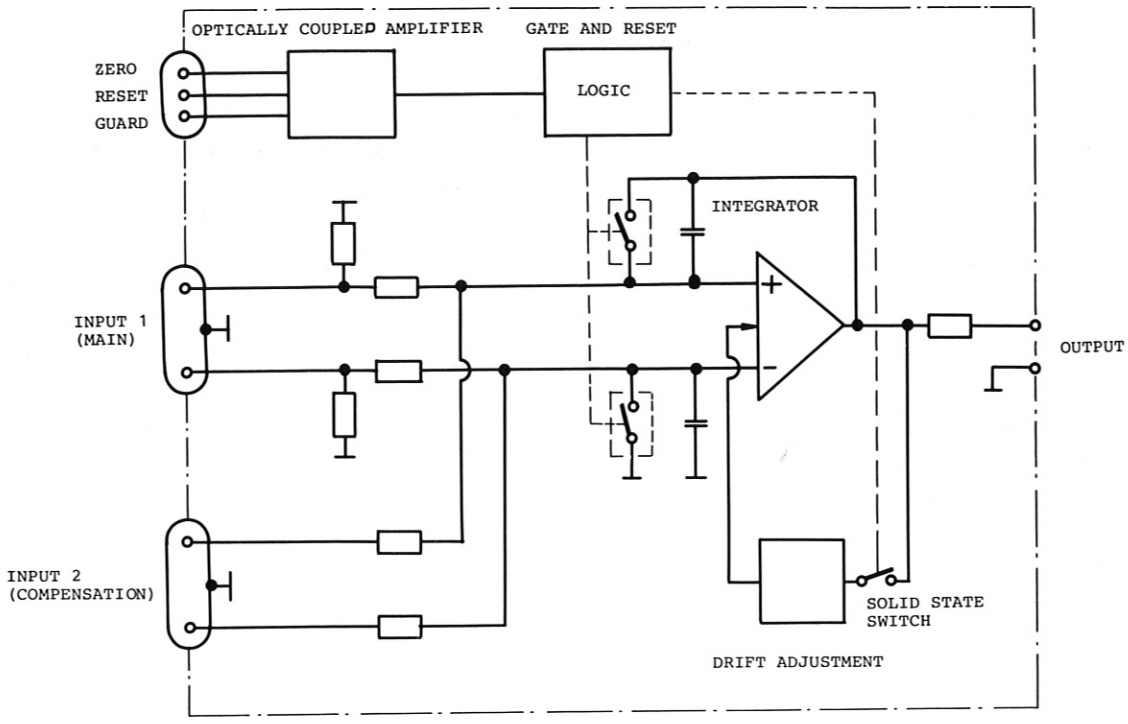

FIG. 37: HIGHLY STABLE ACTIVE INTEGRATOR (DIFFERENTIAL)

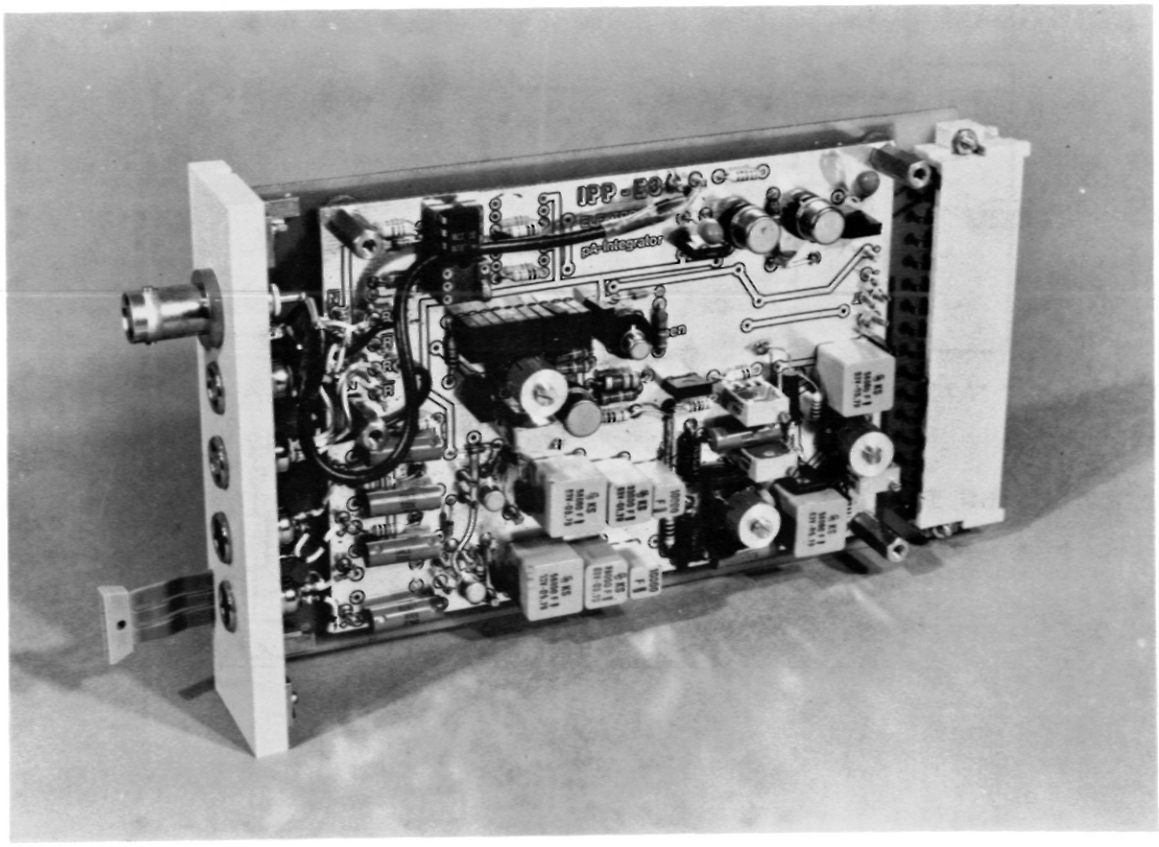

FIG. 38: PHOTOGRAPH OF ACTIVE INTEGRATOR MOUNTED ON EUROPA CRATE (FOR CIRCUIT DESIGN SEE FIG.37)

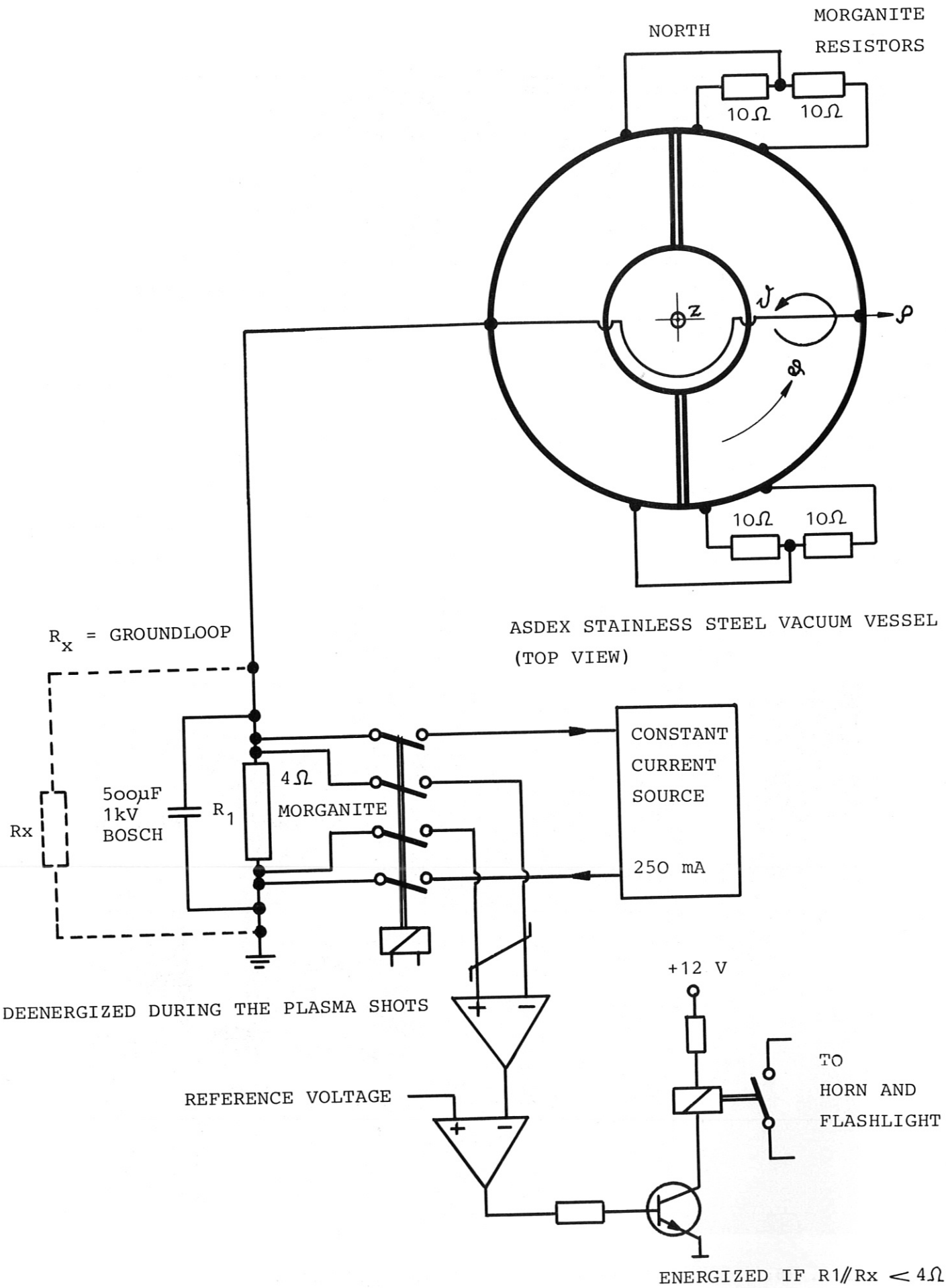

FIG. 39: MEASUREMENT OF GROUND LOOPS AT THE ASDEX VACUUM VESSEL

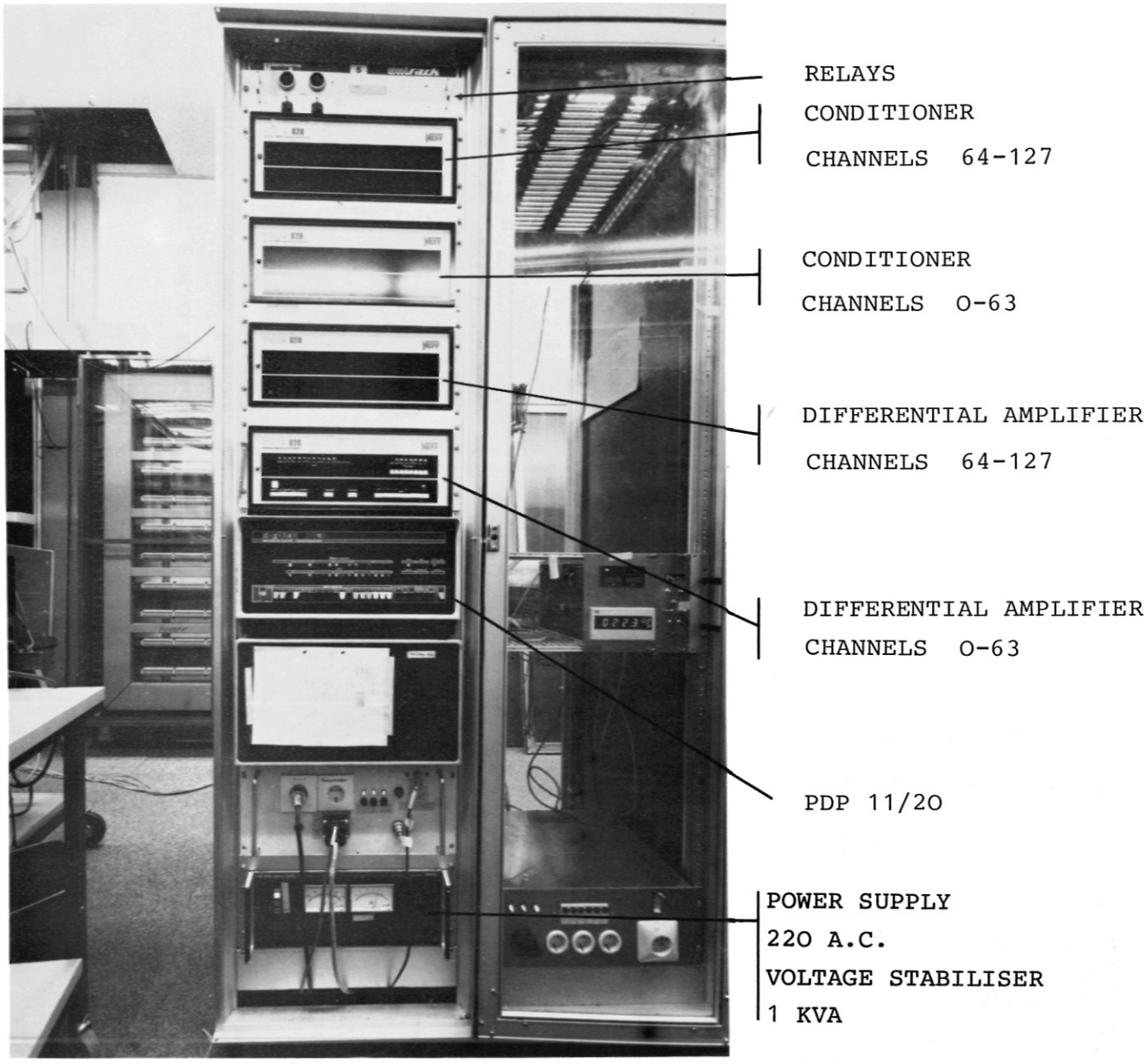

FIG. 40: PHOTOGRAPH OF REAL TIME COMPUTER (PDP 11/20)
AND DATA ACQUISITION SYSTEM MOUNTED IN A RACK
(FOR DESIGN SEE FIG. 42)

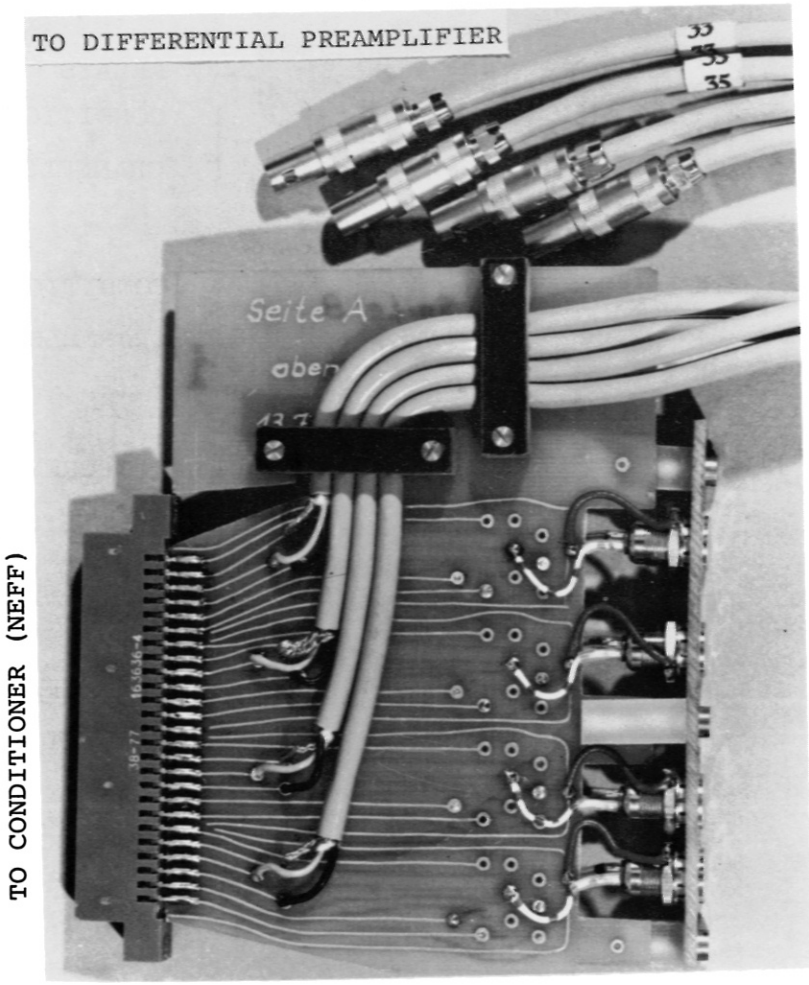

FIG. 41: PHOTOGRAPH OF PRINTED CIRCUIT OF INPUT FOR CONDITIONER UNIT (FOR DESIGN SEE FIG.42)

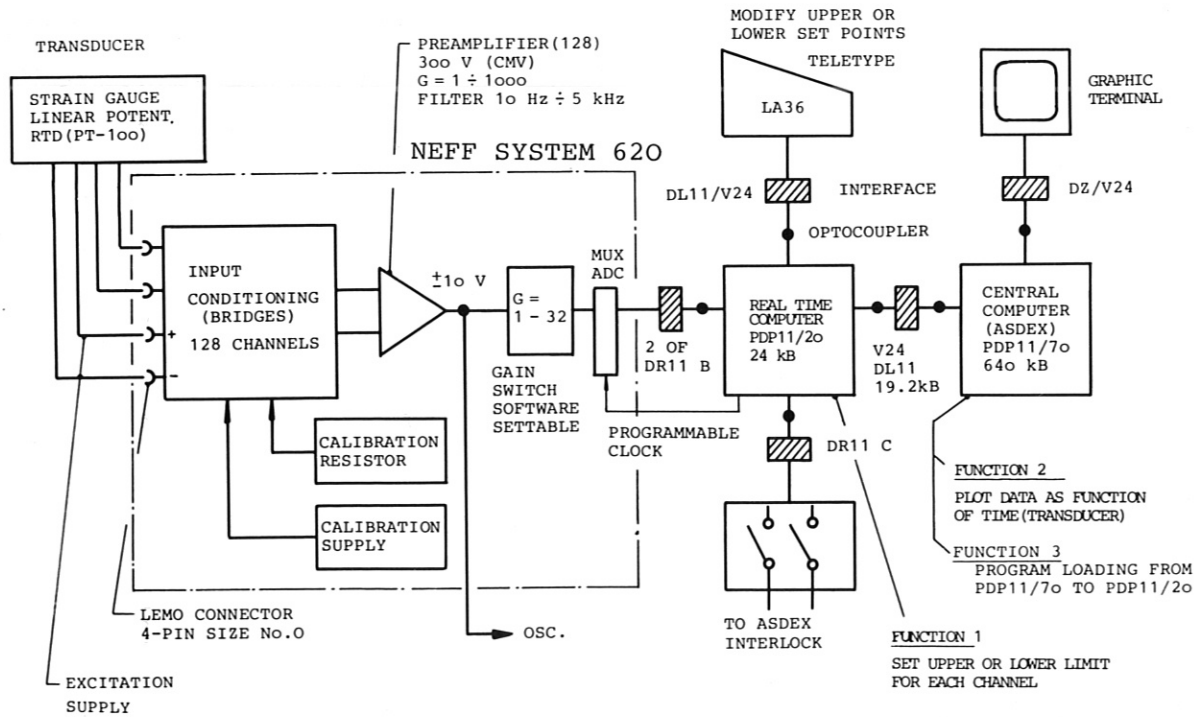

FIG. 42: ASDEX DATA ACQUISITION SYSTEM (NEFF, 620-100/300)
50 kHZ; 12 BIT
128 CHANNELS (2.6 ms PER CHANNEL)

R: MINIMUM UND MAXIMUM GELTEN RELATIV ZU DEM ANGEGEBENEN RUHEWERT,
DER RUHEWERT WURDE AM 31-JUL-80 UM 18:12:09 GEMESSEN.

	KANAL	MINIMUM	MAXIMUM	RUHEWERT	VPRG	VFIX	EICHFAKT
0	LZ....0.4	-0.250 mm	0.250 mm	-0.005	1	20	160.
1	LZ....0.8	-0.250 mm	0.250 mm	-0.013	1	20	160.
2	LZ....012	-0.250 mm	0.250 mm	0.015	1	20	160.
3	LZ....016	-0.250 mm	0.250 mm	-0.013	1	20	160.
4	LZ....M.2	-0.500 mm	0.500 mm	0.000	1	20	160.
5	LZ....M.4	-0.500 mm	0.500 mm	0.000	1	20	160.
6	LZ....M.6	-0.500 mm	0.500 mm	0.007	1	20	160.
7	LZ....M.8	-0.500 mm	0.500 mm	0.015	1	20	160.
8	LZ....M10	-0.500 mm	0.500 mm	0.020	1	20	160.
9	LZ....M12	-0.500 mm	0.500 mm	0.000	1	20	160.
10	LZ....M14	-0.500 mm	0.500 mm	0.000	1	20	160.
11	LZ....M16	-0.500 mm	0.500 mm	0.005	1	20	160.
12	LZ....U.4	-0.250 mm	0.250 mm	-0.010	1	20	160.
13	LZ....U.8	-0.250 mm	0.250 mm	0.000	1	20	160.
14	LZ....U12	-0.250 mm	0.250 mm	-0.025	1	20	160.
15	LZ....U16	-0.250 mm	0.250 mm	0.002	1	20	160.
16	LT....0.1	-1.20 mm	1.20 mm	0.005	1	10	160.
17	LT....0.2	-1.20 mm	1.20 mm	-0.030	1	10	160.
18	LT....0.3	-1.20 mm	1.20 mm	0.005	1	10	160.
19	LT....0.4	-1.20 mm	1.20 mm	-0.020	1	10	160.
20	LT....0.5	-1.20 mm	1.20 mm	-0.025	1	10	160.
21	LT....0.6	-1.20 mm	1.20 mm	0.010	1	10	160.
22	LT....0.7	-1.20 mm	1.20 mm	-0.010	1	10	160.
23	LT....0.8	-1.20 mm	1.20 mm	0.000	1	10	160.
24	LT....0.9	-1.20 mm	1.20 mm	-0.015	1	10	160.
25	LT....010	-1.20 mm	1.20 mm	-0.010	1	10	160.
26	LT....011	-1.20 mm	1.20 mm	0.000	1	10	160.
27	LT....012	-1.20 mm	1.20 mm	-0.040	1	10	160.
28	LT....013	-1.20 mm	1.20 mm	0.000	1	10	160.
29	LT....014	-1.20 mm	1.20 mm	-0.020	1	10	160.
30	LT....015	-1.20 mm	1.20 mm	0.010	1	10	160.
31	LT....016	-1.20 mm	1.20 mm	-0.020	1	10	160.
32	LT....M.1	-2.50 mm	2.50 mm	0.025	1	10	160.
33	LT....M.2	-2.50 mm	2.50 mm	0.020	1	10	160.
34	LT....M.3	-2.50 mm	2.50 mm	0.010	1	10	160.
35	LT....M.4	-2.50 mm	2.50 mm	0.005	1	10	160.
36	LT....M.5	-2.50 mm	2.50 mm	0.050	1	10	160.
37	LT....M.6	-2.50 mm	2.50 mm	0.010	1	10	160.
38	LT....M.7	-2.50 mm	2.50 mm	0.005	1	10	160.
39	LT....M.8	-2.50 mm	2.50 mm	0.005	1	10	160.
40	LT....M.9	-2.50 mm	2.50 mm	0.025	1	10	160.
41	LT....M10	-2.50 mm	2.50 mm	0.010	1	10	160.
42	LT....M11	-2.50 mm	2.50 mm	0.015	1	10	160.
43	LT....M12	-2.50 mm	2.50 mm	0.000	1	10	160.
44	LT....M13	-2.50 mm	2.50 mm	0.010	1	10	160.
45	LT....M14	-2.50 mm	2.50 mm	0.385	1	10	160.
46	LT....M15	-2.50 mm	2.50 mm	0.655	1	10	160.
47	LT....M16	-2.50 mm	2.50 mm	-0.005	1	10	160.
48	LP243RO.1	-1.00 mm	1.00 mm	0.015	1	10	160.
49	LP243RO.3	-1.00 mm	1.00 mm	0.025	1	10	160.
50	LP243RO.5	-1.00 mm	1.00 mm	0.040	1	10	160.
51	LP198RO.7	-1.00 mm	1.00 mm	0.055	1	10	160.
52	LP198RO.9	-1.00 mm	1.00 mm	0.070	1	10	160.
53	LP310RO.1	-1.00 mm	1.00 mm	0.010	1	10	160.
54	LP310RO.3	-1.00 mm	1.00 mm	-0.020	1	10	160.
55	LP310RO.5	-1.00 mm	1.00 mm	0.020	1	10	160.
56	LP288RO.9	-1.00 mm	1.00 mm	0.045	1	10	160.
58	LP.50RO.3	-1.00 mm	1.00 mm	-0.030	1	10	160.
59	LP.50RO.5	-1.00 mm	1.00 mm	-0.035	1	10	160.
60	LP130RO.1	-1.00 mm	1.00 mm	0.015	1	10	160.
61	LP130RO.3	-1.00 mm	1.00 mm	0.065	1	10	160.
62	LP130RO.5	-1.00 mm	1.00 mm	0.015	1	10	160.
63	LP108RO.7	-1.00 mm	1.00 mm	0.080	1	10	160.
64	LP108RO.9	-1.00 mm	1.00 mm	-0.050	1	10	160.
65	LP243RU.1	-1.00 mm	1.00 mm	-0.030	1	10	160.
66	LP243RU.3	-1.00 mm	1.00 mm	-0.020	1	10	160.
67	LP243RU.5	-1.00 mm	1.00 mm	-0.015	1	10	160.
69	LP310RU.1	-1.00 mm	1.00 mm	0.070	1	10	160.
70	LP310RU.3	-1.00 mm	1.00 mm	-0.010	1	10	160.
71	LP310RU.5	-1.00 mm	1.00 mm	0.105	1	10	160.
72	LP310RU.7	-1.00 mm	1.00 mm	0.115	1	10	160.
73	LP310RU.9	-1.00 mm	1.00 mm	-0.115	1	10	160.
74	LP.50RU.1	-1.00 mm	1.00 mm	-0.035	1	10	160.
75	LP.50RU.3	-1.00 mm	1.00 mm	-0.010	1	10	160.
76	LP.50RU.5	-1.00 mm	1.00 mm	-0.050	1	10	160.
77	LP.27RU.7	-1.00 mm	1.00 mm	-0.035	1	10	160.
78	LP.27RU.9	-1.00 mm	1.00 mm	0.015	1	10	160.
79	LP130RU.1	-1.00 mm	1.00 mm	0.105	1	10	160.
80	LP130RU.3	-1.00 mm	1.00 mm	0.110	1	10	160.
81	LP130RU.5	-1.00 mm	1.00 mm	0.110	1	10	160.
82	LP.94RU.7	-1.00 mm	1.00 mm	0.040	1	10	160.
83	LP108RU.9	-1.00 mm	1.00 mm	-0.030	1	10	160.
84	LC265RO.1	-1.00 mm	1.00 mm	-0.080	1	10	160.
85	LC.63RO.1	-1.00 mm	1.00 mm	-0.010	1	10	160.
86	LC265RU.1	-1.00 mm	1.00 mm	-0.120	1	10	160.
87	LC.63RU.1	-1.00 mm	1.00 mm	-0.015	1	10	160.
88	LV273RO.1	-1.00 mm	1.00 mm	0.025	1	10	160.
89	LV273RO.2	-1.00 mm	1.00 mm	0.025	1	10	160.
90	LV273RO.4	-1.00 mm	1.00 mm	-0.475	1	10	160.
91	LV.71RO.1	-1.00 mm	1.00 mm	-0.045	1	10	160.
92	LV.71RO.2	-1.00 mm	1.00 mm	-0.025	1	10	160.
93	LV.71RO.4	-1.00 mm	1.00 mm	0.005	1	10	160.
94	LV273RU.1	-1.00 mm	1.00 mm	-0.020	1	10	160.
95	LV273RU.2	-1.00 mm	1.00 mm	0.005	1	10	160.
96	LV273RU.4	-1.00 mm	1.00 mm	0.010	1	10	160.
97	LV.71RU.1	-1.00 mm	1.00 mm	-0.110	1	10	160.
98	LV.71RU.2	-1.00 mm	1.00 mm	0.000	1	10	160.
99	LV.71RU.4	-1.00 mm	1.00 mm	-0.135	1	10	160.
110	TONNW.O.9	0.000 oC	50.0 oC	23.786	1	100	0.575
111	TONNW.O.8	0.000 oC	50.0 oC	22.674	1	100	0.575
112	TONNW.O.7	0.000 oC	50.0 oC	21.978	1	100	0.575
113	TONNW.O.6	0.000 oC	50.0 oC	23.091	1	100	0.575
115	TONNW.O.4	0.000 oC	50.0 oC	22.674	1	100	0.575
116	TONNW.O.3	0.000 oC	50.0 oC	21.283	1	100	0.575
117	TONNW.O.2	0.000 oC	50.0 oC	21.839	1	100	0.575
118	TONNW.O.1	0.000 oC	50.0 oC	21.004	1	100	0.575
119	TOWNW.U.1	0.000 oC	50.0 oC	24.065	1	100	0.575
120	TOWNW.U.2	0.000 oC	50.0 oC	21.422	1	100	0.575
121	TOWNW.U.3	0.000 oC	50.0 oC	21.422	1	100	0.575
122	TOWNW.U.4	0.000 oC	50.0 oC	21.839	1	100	0.575
123	TOWNW.U.5	0.000 oC	50.0 oC	21.839	1	100	0.575
124	TOWNW.U.6	0.000 oC	50.0 oC	22.117	1	100	0.575
125	TOWNW.U.7	0.000 oC	50.0 oC	22.534	1	100	0.575
126	TOWNW.U.8	0.000 oC	50.0 oC	23.508	1	100	0.575
127	TOWNW.U.9	0.000 oC	50.0 oC	24.899	1	100	0.575

IPP3 GHT 301-80

DISPLACEMENT OF CENTRAL COLUMN (MADE OF WOOD)

DISPLACEMENT OF MAIN FIELD COIL COPPER WINDINGS AND COIL HOUSING (STAINLESS STEEL)

DISPLACEMENT OF INNER OHMIC HEATING COIL AND MAIN FIELD COIL HOUSING

DISPLACEMENT OF DIVERTOR COMPENSATION COIL

DISPLACEMENT OF VERTICAL FIELD COIL

TEMPERATURE OF INNER OHMIC HEATING COIL INSULATION

FIG.43: LIST OF CHANNEL NUMBERS, UPPER AND LOWER SET POINT LIMITS, OFFSET, GAIN AND GAUGE FACTORS FOR REAL-TIME DATA ACQUISITION SYSTEM (FLOW DIAGRAM SEE FIG. 42)

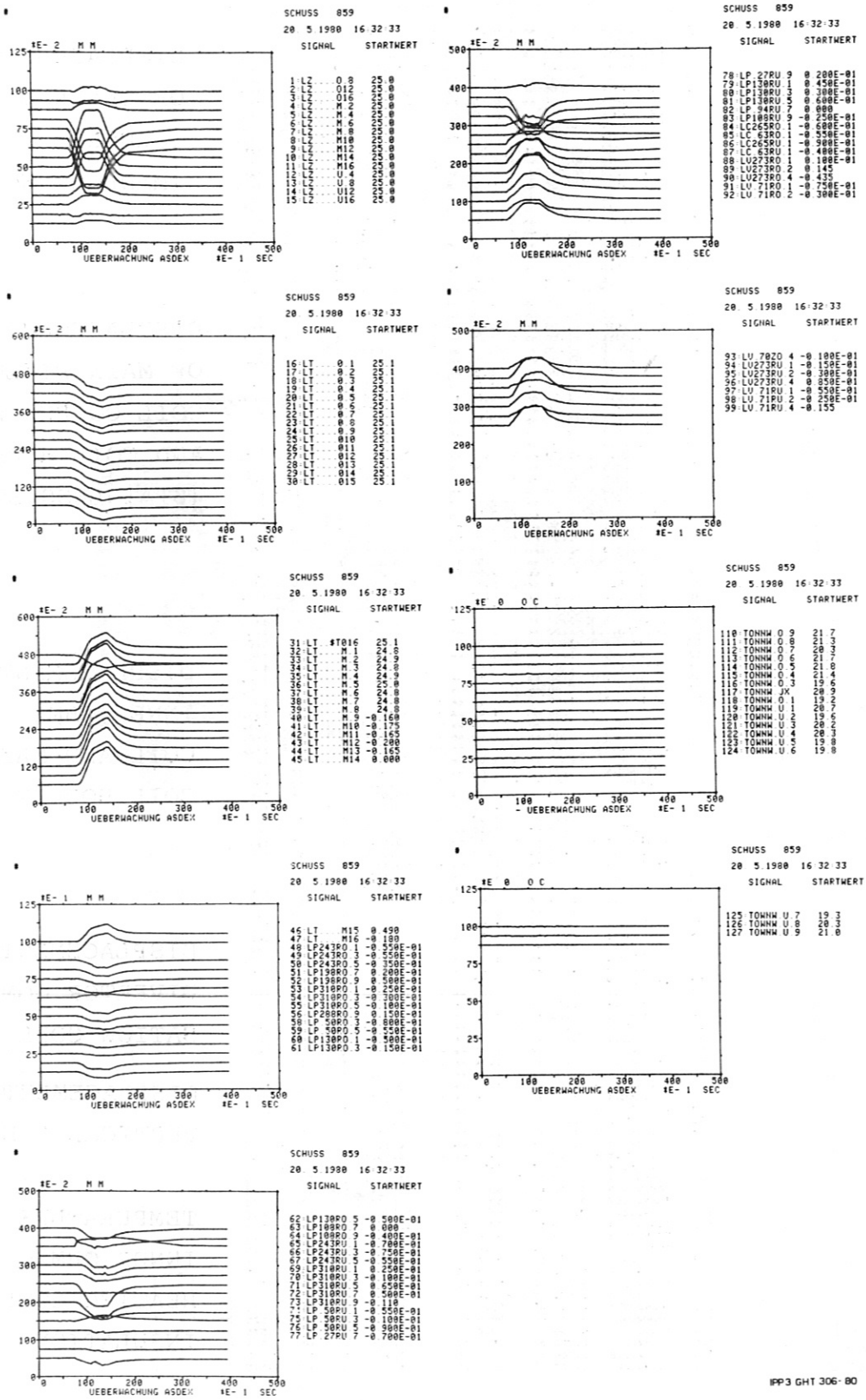

FIG. 44: PLOT DATA OF DISPLACEMENT AND TEMPERATURE OF EACH INDIVIDUAL CHANNEL AS FUNCTION OF TIME (SEE TABLE FIG. 43)